HHS Public Access

Author manuscript

Eur J Med Chem. Author manuscript; available in PMC 2017 December 07.

Published in final edited form as:

Eur J Med Chem. 2016 October 21; 122: 770–785. doi:10.1016/j.ejmech.2016.06.045.

Photosensitizer (PS)-Cyanine Dye (CD) Conjugates: Impact of the Linkers Joining the PS and CD Moieties and Their Orientation in Tumor-Uptake and Photodynamic Therapy (PDT)

Nadine S. James[1], **Penny Joshi**[1], **Tymish Y. Ohulchanskyy**[2,3], **Yihui Chen**[1], **Walter Tabaczynski**[1], **Farukh Durrani**[1], **Masayuki Shibata**[4], and **Ravindra K. Pandey**[1,*]

[1]PDT Center, Cell Stress Biology, Roswell Park Cancer Institute, Buffalo, NY 14263

[2]College of Optoelectronic Engineering, Shenzhen University, Shenzhen, Guangdong, China, 518060

[3]Institute for Lasers, Photonics and Biophotonics, University at Buffalo, Buffalo, NY 14260

[4]Health Informatics, Rutgers School of Health Related Professions, Newark, NJ 07107

Abstract

To investigate the impact of linker(s) joining the photosensitizer HPPH [3-(1'-hexyloxy) ethyl-3-devinylpyropheophorbide-a] and the cyanine dye (CD) in tumor-imaging and photodynamic therapy (dual-function agents), a series of HPPH-CD conjugates were synthesized. The modifications were done in an attempt to minimize Forster Resonance Energy Transfer (FRET) between the two chromophores and maximize singlet oxygen production. Among the conjugates containing variable length of linkers, the HPPH-CD conjugate, in which the photosensitizer (PS) and the CD was joined by four Carbon [$(CH_2)_4$] units showed higher tumor uptake, improved tumor contrast and limited skin uptake in mice bearing Colon-26 (BALB/c) or U87 tumors in Nude mice. The bi-functional agents in which the HPPH was linked at the *meta*-position of phenyl-substituted CD **5, 6** and **7** showed longer tumor response (cure) than the corresponding *para*-substituted analogs **2, 3**, and **4**, which suggests that the orientation of the PS and CD moieties within the conjugate also makes a substantial difference in tumor-specificity. Compared to HPPH, the singlet oxygen yields of all the HPPH-CD conjugates were significantly low, and required a higher therapeutic dose to achieve the same *in vivo* response obtained by HPPH-PDT alone. However, conjugate **6** produced a higher singlet oxygen yield with reduced FRET and exhibited enhanced long-term PDT efficacy in mice bearing Colon-26 (BALB/c) and U87 tumors (nude) than its counterparts, including our lead compound (HPPH-CD), making it the most efficacious of the series. Thus, these conjugates bearing cyanine dye moiety (CD) provide an opportunity of imaging deeply seated tumors for fluorescence-guided surgery with an option of PDT.

Graphical Abstract

Corresponding author: Ravindra K Pandey Ph. D. Ravindra.pandey@roswellpark.org.

Among a series of HPPH (photosensitizer) and CD (near-infrared fluorophore) conjugates, the PS linked with the CD at *meta*-position of the phenyl thioether functionality by four carbon units showed reduced FRET, excellent tumor imaging and photosensitizing efficacy. This approach provides an opportunity to develop efficient dual-function agents for fluorescence guided PDT.

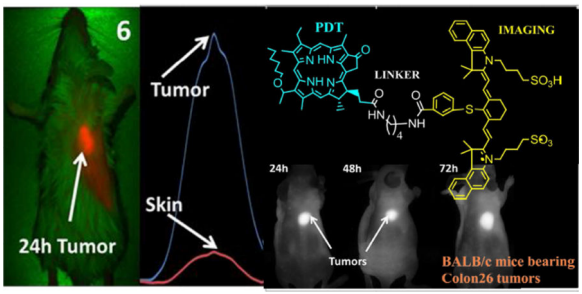

Keywords

Photodyanamic therapy; Forster resonance energy transfer; Photosensitizer; Fluorescence imaging; Dual function agent

INTRODUCTION

One of the main forms of treatment for cancer patients is surgery, and the patient prognosis is generally determined by the precision of surgical resection[1]. Since the intra- operative identification of tumor margins or small foci of cancer cells depends on visual inspection[1], resection may be imprecise and sub-optimal. Given the aggressive and potent nature of brain tumors, identification of new treatment modalities is essential. Numerous studies have shown that malignant brain tumors (gliomas) are generally resistant to treatment via conventional modalities such as surgery, radiation, and chemotherapy[2–5]. Although malignant gliomas have been subjected to aggressive treatments, more than 80 % of them have been observed to recur within 2 cm of the original tumor margin. It is noteworthy, that drugs deemed capable of treating these tumors and diseases of the central nervous system (CNS) are presented with an arduous therapeutic challenge because of the major limitations imposed by the blood-brain barrier (BBB) and systemic toxicity[2,6].

Photodynamic therapy with Photofrin has been used extensively for basic experimental work and clinical brain tumor studies[7]. Other PDT agents, e.g., 5-Aminolevulinic acid (ALA)[7–18] and meta-tetrahydroxy phenylchlorin (m-THPC; Tempoforin, Foscan)[7,19,20] are now employed in photodynamic diagnosis (PDD), fluorescence guided resection (FGR) and intraoperative PDT to treat patients with malignant gliomas. Although, there are variations in the treatment protocol, the photosensitizers used and the light dose delivered pose challenges for a scientific evaluation, there are trends towards the enhanced median survival after a single PDT treatment[16]. Currently FDA-approved PDT agents have certain limitations, such as poor tissue penetration, prolonged time for appropriate accumulation within the tumor versus normal tissue, especially with Foscan, and skin phototoxicity lasting several weeks. With improved agents, the combination of photodiagnosis (PD) or fluorescence guided resection (FGR) with PDT treatment (“see and treat”

approach)[7,10,11,13,17] could offer an intriguing path towards the treatment of several types of tumors. The conjugates discussed herein, combining both photosensitizer (PS) and cyanine dye (CD) moieties, could potentially serve as agents for image-guided therapy of malignant brain and other tumors.

In photodynamic therapy (PDT) there are three essential components which merge to yield the cytoxic agent, singlet oxygen ($^1O^*_2$), that ablates tumor tissue. These components are the photosensitizer (PS), appropriate wavelength of light and molecular oxygen (O_2). PS in the ground state is immediately excited to a short lived specie in the singlet state ($^1PS^*$) when it absorbs light of a particular wavelength. The singlet state rapidly converts to an excited triplet state ($^3PS^*$) through the process of intersystem crossing (ISC). There are three pathways by which PDT occurs. These are types I – III but the dominant pathway is Type II, whereby the $^3PS^*$ transfers energy to the molecular oxygen within tissue, resulting in the generation of reactive oxygen species (ROS), specifically, the oxygen molecule in the excited state, singlet oxygen ($^1O_2^*$),[21–26] Figure 1. Sufficient $^1O_2^*$ generation leads to the irreversible destruction of diseased tissues without affecting surrounding healthy ones[21–26]. Systemically, PDT is also capable of the destruction of tumor tissue by invoking an immune response and vascular shutdown of the blood vessels surrounding the diseased tissue[21–26].

We have previously shown that the HPPH-CD conjugate, prepared by reacting HPPH with an amino-functionalized cyanine dye (CD) **1** (Figure 2) can be used for tumor-imaging and imaging guided PDT [27,28] in tumored mice. However, it was found that the generation of singlet oxygen ($^1O_2^*$) and the corresponding PDT efficacy of the PS moiety in the conjugate was compromised due to the competing pathways, including electronic excitation energy transfer from PS moiety to CD moiety (i.e., Forster Resonance Energy Transfer, FRET) [27–29].

In FRET, the excited singlet level of **π**-electron system of PS moiety is deactivated by transferring energy to CD moiety, instead of undergoing intersystem crossing to populate its triplet level. The reduced PS triplet yield, in turn, results in a decrease in $^1O_2^*$ production and, correspondingly, impairs a long-term tumor cure[27–29]. In other words, FRET caused the excitation of HPPH, the energy donor, to be partially transferred to the fluorophore, the energy acceptor, instead of molecular oxygen, resulting in reduced singlet oxygen production. The main objective of present study was to synthesize a series of HPPH-CD conjugates **2–7** (Scheme 2) joined together with variable length of linkers/orientations, and investigate the impact of such alterations in photophysical properties (e. g., FRET, singlet oxygen production) fluorescence imaging ability, tumor-uptake and long-term tumor response by PDT.

Herein, we report the synthesis, molecular modeling, photophysical properties, intracellular localization, *in vitro* and *in vivo* tumor-uptake, *in vivo* imaging, and the PDT efficacy of PS-CD conjugates **2–7**.

RESULTS AND DISCUSSION

Chemistry

To investigate the impact of the length of linkers joining PS and CD in tumor imaging and photosensitizing efficacy of the conjugates, the lead conjugate **1** and a series of related analogs **2–7** were prepared by following the methodology depicted in Scheme 1. In brief, the carboxylic acid functionality at position 17^2- of the HPPH was reacted with mono-amine protected diamines containing 2, 4 and 6 carbon units. The amine functionalized HPPH derivatives were individually reacted with the cyanine dyes **11** and **12** bearing a carboxylic acid functionality either at *para*- or *meta*-position of the phenyl ring and were obtained in moderate yields.

Optical spectroscopy

For all the HPPH-CD conjugates, the optical absorption spectra include a characteristic absorption of HPPH (long wavelength peak at ~664 nm) and that of CDs (long wavelength absorption in the range of 838 – 840 nm) (Figure 3A). Hence, the spectral positions of the corresponding absorption bands for HPPH and CD moieties do not shift noticeably when linked within conjugate, suggesting that their TT-electron systems are not significantly affected by conjugation. This was expected as these non-conjugated TT-electron systems are relatively distant from each other; similar pattern has also been observed for other types of conjugates of PS (HPPH) and CD[30–32]. The excitation of HPPH moiety of the conjugates **2–7** produced fluorescence from the HPPH (peaked at ~666 nm) as well as the CD moieties (maxima at ~875–878 nm) (Figure 3B). The fluorescence of HPPH moiety is evidently less quenched for **3** and **6** (i.e., HPPH fluorescence for **3** and **6** are most intense among those of all conjugates), despite that corresponding HPPH absorption bands ($\lambda_{max} \approx 664$ nm) for the same samples of **3** and **6** are, in fact, least intense among all (Figure 3A). This observation points to that electronic excitation energy transfer between HPPH and CD moieties in **3** and **6** is least efficient among all studied compounds. As we have demonstrated in our earlier work[30–32] quenching of PS fluorescence in similar PS-containing conjugates correlates with a decrease in singlet oxygen production by PS and indeed occurs due to FRET within the conjugates, where the HPPH moiety acts as a donor and the CD is an acceptor. This phenomenon for similar system of PS conjugated with another chromophore has been shown by another group.[29]

Singlet oxygen, $^1O_2{}^*$, a key cytotoxic agent in PDT is produced by interaction of the molecular oxygen, $^1O_2{}^*$, in its ground triplet state, with the triplet excited state of the PS molecule, which is excited through intersystem crossing from the excited singlet state of PS [21–26]. This infers that if the excited singlet state of PS is deactivated through a transfer to the CD moiety, instead of intersystem crossing to PS triplet state, the $^1O_2{}^*$ generation by PS is reduced[23]. To compare the production of singlet oxygen by HPPH moiety within conjugates and that by free HPPH, we have performed a time-resolved spectroscopy of the singlet oxygen phosphorescence peaked at ~1270 nm. In these experiments, amount of the produced $^1O_2{}^*$ was evaluated by the decay of its phosphorescence.

Since this decay is in microsecond range (for water or alcohol-based environment) it is possible to resolve singlet oxygen emission, distinguishing it from other signals coming to detector (e.g., scattered excitation light and fluorescence emission) and quantify singlet oxygen generation, as described previously[22,24,30,31]. Briefly, area under every decay curve of $^1O_2$ phosphorescence was integrated and singlet oxygen yield for every sample compound was determined by comparison of the integrated area value with that obtained for reference compound with known $^1O_2$ yield (e.g., HPPH with $^1O_2$ yield of ~45%[32].

As one can see in Figure 4, the generation of $^1O_2^*$ by the HPPH moiety in all conjugates is significantly reduced in comparison with HPPH alone, similarly to fluorescence intensity (Fig. 3B). It is worth, however, noting that $^1O_2^*$ yields for compounds **3** and **6** are noticeably higher than those for other conjugates, which correlates with more intense fluorescence from their PS moieties (Fig. 3B) and suggests that FRET between PS and CD moieties is less pronounced in **3** and **6** than in other conjugates.

Flow Cytometry: Uptake of the Conjugates by Colon-26 and U87 Cells

The *in vitro* cell uptake of the conjugates **2–7** in both Colon-26 and U87 cell lines was determined by flow cytometry. The results summarized in Figure 5 suggest that the conjugates **3** and **6** in which the HPPH and CD moieties are linked with 4 carbon units show 8 – 10 fold higher uptake than the conjugates **2, 5** (HPPH and CD are linked with 2 carbon units) and **4, 7** (HPPH and CD are linked with 6 carbon units).

The disparity in uptake of the medium linked compounds versus those with the short and long linkers could be due to the difference in rate of binding to the cellular membranes and/or the rate of diffusion and endocytosis for the individual conjugate[33].

***In vivo* fluorescence imaging—**For determining the fluorescence imaging potential of the conjugates **2–7**, these compounds were individually injected intravenously (i.v.), at a drug dose 0.03 μmol/kg, in BALB\c mice bearing Colon-26 tumors (3 mice/group). The tumor and skin of each mouse was imaged at 24 h, 48 h, and 72 h post injection (p.i.) in a Maestro GNIR Flex *In-Vivo* imaging system using a broadband excitation at 710 – 740 nm and an 800 long pass emission. The mice (mice/group) were sacrificed at each time point (24h, 48h and 72h) and the organs were imaged *ex vivo*.

Imaging each organ separately (*ex-vivo*) showed a significant uptake of the conjugates in liver (not observed during whole body imaging), which could be the main route of clearance of the compounds from the system as reported for most of the porphyrin-based PDT agents[34,35]. The tumor vs. skin uptake of mice with conjugates **2–7** are tabulated in Figure 6. The imaging potential of conjugate **6**, one of the most promising candidates was also investigated in nude mice bearing U87 glioblastoma tumors under similar imaging parameters. The mice were imaged at 24 h, 48 h, and 72 h post injection (p.i), and the tumor-images are illustrated in Figure 7. As can be seen, similar to mice bearing Colon-26 tumors, conjugate **6** also showed a significant retention in U87 tumor at 24, 48 and even at 72h post-injection.

***In vitro* and *in vivo* photosensitizing efficacy—**MTT cell viability assays were conducted on **2–7** using the Colon-26 carcinoma cell line in two independent experiments with triplicates in each experiment. The plates were irradiated with a fluence of 4 J/cm^2 and fluence rate of 3.2 mW/cm^2 after 24 h incubation with the compounds. The *in vitro* PDT efficacy was investigated 48 h post-irradiation and the EC_{50} values were determined. The conjugate bearing a medium length of linker showed improved photosensitizing efficacy, and the following pattern was observed Medium linker (**3**, EC_{50} 0.13 μM and **6**, EC_{50} 0.18 μM) > long linker (**4**, EC_{50} 0.72 μM and **7**, EC_{50} 0.2 μM) > short linker (**2**, EC_{50} 2.51 μM and **5**, EC_{50} 1.58 μM) conjugates. Overall, the *meta*-linked conjugates appeared to be more effective *in vitro* than their corresponding *para*- linked counterparts with a slight difference in the case of the conjugates bearing medium linkers, Figure 8A. Using the standard protocol, the *in vivo* efficacy of the conjugates was initially evaluated in 6–7 week BALB/c mice bearing Colon-26 tumors (size: 4–5 mm) drug doses. The tumors were exposed to a laser light (665 nm, 128 J/cm^2 and 14 mW/cm^2) at 24 h post-injection, at variable drug doses and the tumor-regrowth was monitored daily. The mice with no tumor-regrowth were kept for a longer period of time (60 days), and those with tumor regrowth of >400 mm were euthanized. The results obtained from the HPPH conjugates in which the HPPH and CD moieties are linked with long, medium and short alkyl chain linkers are summarized in Figure 8B. tumors (size: 4–5 mm) drug doses. The tumors were exposed to a laser light (665 nm, 128 J/cm^2 and 14 mW/cm^2) at 24 h post-injection, at variable drug doses and the tumor-regrowth was monitored daily. The mice with no tumor-regrowth were kept for a longer period of time (60 days), and those with tumor regrowth of >400 mm were euthanized. The results obtained from the HPPH conjugates in which the HPPH and CD moieties are linked with long, medium and short alkyl chain linkers are summarized in Figure 8B.

As can be seen, at a higher dose (3.5 μmol/kg), the long linker conjugates **4** and **7** were quite effective, but lowering the dose also reduced the long-term PDT response. In order to compare the efficacy of the conjugates, the long-term PDT response was determined at drug doses (0.4, 0.75, 1.5, 2.5, and 3.5 μmol/kg) at a fluence of 128 J/cm^2 and fluence rate of 14 mW/cm^2. Compounds **2** and **5** were too toxic at the doses of 3.5 or 2.5 μmol/kg and the mice either died or demonstrated morbidity and were euthanized. At a dose of 0.4 μmol/kg, no tumor response was observed. However, conjugate **5** at 1.5 μmol/kg showed 80% cure (8/10 mice were tumor-free, Figure 8B). The deaths caused by the compounds, especially the short linked compounds could be due to liver phototoxicity. When the long linker conjugates **4** and **7** were assessed at 1.5 and 0.75 μmol/kg doses, significant tumor cure was observed (Figure 8B). In the case of the conjugates with medium linkers **3** and **6** at a dose of 1.5 μmol/kg produced 20% (2/10 mice) and 80% (8/10 mice) tumor-free mice respectively.

Similar *in vitro* and *in vivo* studies with conjugates **2–7** were also performed using U87 tumor cells. The plates were irradiated with a fluence of 4 J/cm^2 and fluence rate of 3.2 mW/cm^2 after 24 h incubation with the compounds. MTT was done at 48 h post-irradiation. The *in vitro* response of conjugates **2–7** is illustrated in Figure 9A. The EC_{50} values of the conjugates were compared, and the *in vitro* phototoxicity followed the following order: Conjugates with medium linkers (**3**, EC_{50} 0.29 μM and **6**, EC_{50} 0.15 μM) > longer linker (**4**, EC_{50} 0.59 μM and **7**, EC_{50} 0.38μM) > short linker (**2**, EC_{50} 0.79 μM and **5**, EC_{50} 0.57 μM).

Similar to the results shown in the Colon-26 cell line, the meta-linked conjugates appeared to be more effective *in vitro* than their *para*- linked counterparts in the U87 cell lines.

We also extended this study to investigate the utility of the conjugates **4** and **6** (showed the best response in mice bearing Colon-26 tumors) in treating nude mice bearing U87 tumors under similar treatment parameters. From the data illustrated in Figure 10, it can be seen that both the conjugates produced limited activity. However, compared to compound **4**, the conjugate **6** showed a significant delay in tumor re-growth. The limited PDT efficacy of a variety of porphyrin-based compounds in immune depressant mice have also been investigated in several laboratories demonstrating a significantly low long-term tumor cure, further confirming that adaptive immune response plays an important role in PDT outcome.[36–38]

It is well established that for a photodynamic process to occur, three critical elements are necessary: (a) photosensitizer (drug), (b) light and (c) oxygen. In a photodynamic therapy process, excitation of the photosensitizer (present in tumor) converts the molecular oxygen (also present in tumor) to singlet oxygen (a cytotoxic agent), which destroys the blood vessels (besides other complex processes) and tumor(s) starve to death. In general PDT is extremely effective for treating highly vascularized tumors, which could be due to higher uptake of the photosensitizer and increased oxygen availability. Therefore, to establish a correlation between the vascularity and PDT efficacy, the estimates of vascularity in both Colon-26 and U87 tumors were determined by histopathology analysis.[41,42]

The results depicted in Figure 11 clearly indicate that both tumor types are highly vascularized, homogeneous with leaky vessels. Thus, these tumors should have similar uptake of the photosensitizer and oxygen. The limited long-term PDT cure of U87 tumors implanted in immune-compromised nude mice could possibly be due to adaptive immune response, which is known to play an important role in PDT outcome.

Intracellular Localization of the Conjugates in Colon-26 and U87 Cells

It has been shown by us and others that subcellular localization of the photosensitizer(s) plays a key role in PDT efficiency, as well as direct induction of cell death *via* apoptosis, autophagy or necrosis.[43,44] Predominant localization of the PS to the mitochondria initiates cell death via apoptosis[45,46], whereas, lysosomal or plasma membrane localization can induce either a necrotic or an apoptotic cell death pathway.[45]

To determine whether the variability in the *in vitro* and *in vivo* phototoxicity of the conjugates with various linkers correlates with the intracellular localization of the compounds in our studies, the localization of conjugates **2–7** at variable concentrations was assessed in Colon-26 and U87 cells, (Figure 11B) at variable concentrations using organelle-specific dyes MitoTracker Red and FluoSpheres ® yellow green as well-known probes for the mitochondria and the lysosome respectively. From the results (false color images) summarized in Figure 11A and 11B it can be seen that conjugate **6** predominantly localized in the mitochondria in Colon-26 and U87 tumors. Likewise, all the conjugates in the series predominantly show mitochondrial localization (confirmed by color overlay), supplemental data Figures S39 to S46.

Numerous studies have shown that localization of the PS to the mitochondria[44,47] or to the cell nucleus[48] elevates the phototoxicity compared to localization in other sites. Mechanistically, such localization within the mitochondrial membrane can cause the disruption of the anti-apoptotic protein complex, such as Bcl-2 and Bcl-xL[44,49] by inhibition following PDT treatment. A cascade of events then leads to the manifestation of apoptotic cell death. However, these conjugates were not subjected for such a detailed study.

Molecular Modeling of Linked Conjugates

In order to examine the effects of linker length and substituent position (meta vs. para) on the structures of the conjugates, the 3 dimensional models of the conjugates **2–7** were built with Tripos SYBYLX 1.1 molecular modeling software using standard geometry and energy optimized with the Semi empirical MO, PM3. The conformational search for each conjugate was performed with molecular modeling software MOE 2011.10 using both stochastic Monte Carlo and Molecular Dynamics with the modified MMFF94s force field. Although the exhaustive conformational search was not performed, it became evident that the flexibility of the linker and other parts of the conjugates allow them to explore a large conformational space during our conformational searches. In other words, the conjugates are not rigid and contain many rotatable dihedral angles including the ones in the linker regions. As a result, these flexible torsional angles allow the conjugates to assume many different conformations

No outstanding conformations that could explain the difference in activity of the conjugates were observed for either the substituent positions (*meta*- vs *para*-) or the linker length. Some of the conformations observed are shown in Figure 12. It is clear that the regardless of the linker length or the substituent position, the flexibility of the conjugates allows two chromophores to be in close proximity that allows for energy transfer between two moieties, explaining the quenching observed for fluorescence and reduced singlet oxygen generation from the HPPH moiety (Figure 3, 4). Although the remarkable advantage in uptake for the medium sized linker conjugates, **3** and **6**, over short, **2** and **5**, and long linker conjugates, **4** and **7**, shown by the flow cytometry, there were no specific structural features found for the medium sized linker conjugates that supported the flow cytometry data. Thus it is either due to simple hydrophobicity or alternatively the affinity to specific membrane transporter, but the modeling study alone cannot elucidate specific rational for the observed difference. This significant difference in cellular uptake might play a role in *in vitro* PDT efficacy, but additional factors seem to play more important role in *in vivo* efficacy.

CONCLUSIONS

A series of conjugates, similar to our lead conjugate (HPPH-CD), were synthesized by varying; (1) the length that links the two moieties, from two to six carbon units and (2) the intramolecular orientation of the photosensitizer with respect to the fluorophore in the *para*- or *meta*-position. The results obtained from a series of HPPH-CD conjugates suggest that the orientation of the two chromophores linked by variable lengths of carbon units made significant difference in *in vivo* PDT efficacy. All the conjugates were predominantly localized in the mitochondria. The conjugates that were linked in the meta-position (**5, 6** and

7) of phenyl substituted CD showed enhanced *in vitro* and *in vivo* activity than the corresponding *para*-linked analogs (**2, 3** and **4**) in most cases. Although, all the conjugates appeared to localize in the mitochondria, conjugates **3** and **6**, linked in the *para* and *meta*-position, respectively, where the photosensitizer and the cyanine dye moieties were joined with a four carbon unit linker, produced 8- to 10- fold higher tumor uptake resulting in improved tumor contrast. Among all the conjugates (including the lead candidate **1**) conjugate (**6**) exhibited slightly increased single oxygen yield, when compared to that of HPPH, and long-term PDT efficacy (tumor cure) in mice bearing Colon-26 (BALB/c) and U87 tumors (nude) making it the most photoactive of the series. On the other hand, the conjugate with two carbon units (**2**) in the *para*- position was the least photoactive within the series. Molecular modeling study suggested that regardless of the linker length or its position, the flexibility of linkers in the conjugates allowed the two ring systems to be in proximity which might be facilitating energy transfer between the two moieties, and needs further in depth study. Further studies to understand the reason for the difference in activity of conjugates **2** (least photoactive) versus **6** (most photoactive) in this and other tumor models are currently underway.. All conjugates showed significant quenching of the CD moiety, and it was minimal in conjugate **6** in which HPPH was conjugated with phenyl substituted CD at the *meta*- position. Replacing the flexible linkers with non-conjugated rigid moieties may help in developing desired compounds with reduced quenching of singlet oxygen[29]. The syntheses of such analogs are currently underway.

METHODS AND EXPERIMENTAL

In vitro studies

(1) *In vitro* tumor cell uptake, (2) cell phototoxicity assay and (3) intracellular localization tumor models: Colon-26 and U87.

In vivo studies

(1) *In vivo* tumor uptake, (2) *in vivo* PDT efficacy and (3) *in vivo* imaging tumor models: BALB/c mice inoculated with Colon-26, and nude mice with U87.

Chemistry

All reagents mentioned herein were purchased from Sigma Aldrich® and used without further purification. Photophysical experiments were carried out using spectroscopic grade solvents. The reactions were monitored by this layer chromatography (TLC) and/or spectrophotometrically. TLC was done on ANALTECH pre-coated silica gel GF PE sheets (Cat. 159017, layer thickness 0.25 mm). Purification was done by flash column chromatography performed over Silica Gel 60 (230 – 400 mesh). Preparative TLC plates were also used, in some cases, for the purification (ANALTECH precoated silica gel GF glass plate, Cat. 02013, layer thickness 1.0 mm). Dichloromethane was dried over phosphorous pentaoxide (P_2O_5) under N_2 atmosphere. The synthetic intermediates and the final products were characterized by NMR (400 MHz) and mass spectrometry (HRMS). NMR spectra were recorded on a Varian 400 MHz spectrometer in 1:1 ratio of CD_3OH to $CDCl_3$ at 298 K for the conjugates and in DMSO-d_6 solution at 308 K and referenced to residual $CDCl_3$ (7.26 ppm) or DMSO-d_6 (2.50 ppm). EI-Mass spectra were carried out on a

Brucker Esquire ion-trap mass spectrometer equipped with a pneumatically assisted electrospray ionization source, operating in positive mode. UV-Visible spectrums were recorded on Varian Cary 50 Bio UV-Visible spectrophotometer using dichloromethane or methanol as solvent.

3-[1'-hexyloxyethyl]-3-devinylpyropheophorbide-*a* (HPPH) was synthesized after many steps following the extraction of its precursor, crude chlorophyll-*a*, from *Spirulina Pacifica Algae*[32]. HPPH was linked to various aliphatic N-BOC-protected amines via a peptide linkage. Upon de-protection these were conjugated to the commercially available near infrared fluorophore (IR 820) upon modification with 3-mercaptobenzoic acid or 4-mercaptobenzoic in our laboratory. After obtaining the respective dyes the conjugates with varying linkers were synthesized. All reagents used for the synthesis of the desired conjugates were purchased from Sigma Aldrich, USA. The intermediates and the final compounds were characterized by NMR spectroscopy, HRMS, and UV-Vis. Purification was done by flash column chromatography.

Compound 2—HPPH-N-Boc ethylenediamine (35.0 mg, 0.052 mmol) was taken in a dry round bottom flask (RBF) (50.0 ml) and stirred with 50% trifluoroacetic acid (TFA) in dichloromethane (DCM) (5.0 ml) at RT for 3 hr. The reaction mixture was concentrated and dried under high vacuum to remove trace of TFA. The crude thus obtained was dissolved in anhydrous DMF (25 ml) and CD4COOH (50.0 mg, 0.052 mmol), Benzotriazol-1-yloxy)tris(dimethylamino)phosphonium hexafluorophosphate (BOP), 30.0 mg (0.067 mmol) and triethyl amine (3–4 drops) were added and the reaction mixture was stirred for 12 hr at room temperature under Argon atmosphere. Solvent was removed under vacuum and the product was purified over preparative plates using 15 % methanol-dichloromethane to give the final product, black solid, in a 35% yield. UV-Vis λ_{max} (in MeOH): 838.9 nm (ε 2.04 × 10^5), 659.9 nm (ε 5.13 × 10^4), 607.0 nm (ε 1.16 × 10^4), 538 nm (ε 1.0 × 10^4), 408 nm (ε 8.1 × 10^4); ^{1}H-NMR (400MHz, CD_3OD, δ ppm): 9.76 (s, 1H, H-5 of HPPH), 9.34 (br s, 1H, H-10 of HPPH), 8.50/8.51 (d, 2H, for −CH=C<u>H</u>-C=C-C=C<u>H</u>-CH=C-, *J*=14.1 Hz), 8.44/8.43 (s, 1H, H-20 of HPPH), 7.64–7.80 (cm, 8H, 2H for phenyl thioether aromatic protons & 6H for cyanine dye aromatic protons), 7.46 (d, 2H, cyanine dye aromatic protons, *J*=7.5 Hz), 7.2–7.4 (cm, 4H, 2H for cyanine dye aromatic protons & 2H for phenyl thioether aromatic protons), 7.16 (dd, 2H, cyanine dye aromatic protons, *J*=8.3, 3.2 Hz), 6.77 (m, 2H, −C<u>H</u>=CH-C=C-C=CH-C<u>H</u>=C-), 5.92 (m, 1H, H-3^1 of HPPH), 5.00–5.15 (m, 2H, 13^1-CH_2 of HPPH), 4.7 (4H, –NC<u>H</u>$_2$$(CH_2)_3SO_3$), 4.29 (q, 1H, H-18 of HPPH, *J*=7.0 Hz), 3.95 (br m, 1H, H-17 of HPPH), 3.55–3.80 (overlapped m, 7H, ring-CH_3, 8-C<u>H</u>$_2$$CH_3$, & -OC<u>H</u>$_2$$(CH_2)_4CH_3$ of HPPH), 3.34 (s, 3H, ring-CH_3,), 3.22 (s, 3H, ring-CH_3), 2.6–2.8 (cm, 12H, 4H for cyclohexene C<u>H</u>$_2$$CH_2$C<u>H</u>$_2$, 4H for -N$(CH_2)_3$C<u>H</u>$_2$$SO_3$, 4H for −NH(C<u>H</u>$_2$$)_2$NH-), 2.42, 2.23, 2.05 (3× m, 4H for 17 -CH_2CH_2CO-), 2.12 (d, 3H, 3^1-CH_3, *J*=6.6 Hz), 1.57–1.78 (overlapped m, 17H, 3H for 18-CH_3 of HPPH, 12H for 4× CH_3 of cyanine dye, 2H for -OCH_2C<u>H</u>$_2$$(CH_2)_3CH_3$ of HPPH), 1.54 (t, 3H, 8-CH_2C<u>H</u>$_3$, J=6.9 Hz), 1.1–1.5 (overlapped m, 12H, 2H for cyclohexene CH_2C<u>H</u>$_2$$CH_2$, 8H for 2 x–N$CH_2$(C<u>H</u>$_2$$)_2$ CH_2SO_3-, 2H for $CH_2)_2$C<u>H</u>$_2$$(CH_2)_2$ CH_3 of HPPH), 1.18 (m, 4H, -O$(CH_2)_3$(C<u>H</u>$_2$$)_2CH_3$ of HPPH), 0.71 (m, 3H, -O$(CH_2)_5$ C<u>H</u>$_3$ of HPPH). ^{13}C-NMR (100MHz, $CDCl_3$ / CD_3OD, δ ppm): 173.9, 172.4, 149.4, 145.2, 145.0, 141.5, 139.2, 136.4, 133.7, 133.6, 131.8, 130.6, 129.9, 128.5, 127.9,

127.7, 125.4, 125.1, 122.0, 110.3, 104.1, 100.8, 97.7, 92.9, 72.78/72.82, 69.7, 51.7, 51.0, 46.2, 44.2, 31.7, 30.1, 27.3, 27.18/27.21, 26.4, 26.3, 25.98/26.00, 24.5, 24.4, 22.9, 22.5, 22.3, 19.4, 17.3, 13.8, 11.9, 11.2, 10.84/10.86, 8.4. Mass: m/z calculated for $[M+H^+]$ $C_{94}H_{107}N_8O_{10}S_3$: 1605.7204, found HRMS $[M+H]^+$: 1605.7462.

Conjugate 3—HPPH-1,2-butanediamine (41 mg, 0.0559 mmoles), CD_4COOH (28 mg, 0.02795 mmoles), BOP (16 mg, 0.03634 mmoles) and 3 drops triethyl diamine were combined with 10 ml anhydrous DMF in a two neck RBF under Argon atm. Mixture was stirred at room temperature for 12 h. Upon completion the reaction mixture was neutralized with 5 % acetic acid and DMF was removed by concentrating the mixture under high vacuum. The resultant slush was re-suspended in DCM and washed with brine (×3) the aqueous layer was washed with DCM until it was transparent. All the organic layers were combined, dried over Na_2SO_4 and concentrated under high vacuum. This was purified via flash column chromatography using a gradient of 5 – 20% MeOH/DCM to yield a black solid (Pure yield 42 %). UV-Vis λ_{max} (in MeOH): 839 nm (ε 9.75×10^4), 661 nm (ε 4.14×10^4), 606.1 nm (ε 9.75×10^3), 537.1 nm (ε 9.75×10^3), 502 nm (ε 9.75×10^3), 502 nm (ε 1.06×10^4), 407.9 (ε 7.65×10^4); ^{1}H-NMR (400MHz, DMSO-d_6, δ ppm): 9.80/9.79 (s, 1H, H-5 of HPPH), 9.74 (s, 1H, H-10 of HPPH), 8.78 (s, 1H, H-20 of HPPH), 8.65 (d, 2-CH = (CH-C=C-C=CH-CH=C-, *J*=14.1 Hz), 7.30–8.30 (8 × m, 18H, 2H for −NH(CH_2)$_4$NH-,12H for cyanine dye aromatic protons & 4H for phenyl thioether aromatic protons), 6.39 (d, 2H,-CH=CH-C =C-C=CH-CH=C-, *J*=14.2 Hz), 5.97 (m, 1H, 3^1-H of HPPH), 5.05, 5.19 (2 × d, each 1H, 13^1-CH_2 of HPPH), 4.51 (m, 1H, 18-H of HPPH), 4.20–4.30 (m, 5H, 1H for 17-H of HPPH, 4H, 2 × – −NCH_2(CH_2)$_3$$SO_3^-$), 3.65–3.80 (m, 4H, -OC$H_2$($CH_2$)$_4$$CH_3$ & 8-C$H_2$$CH_3$ of HPPH), 3.22, 3.36, & 3.63 (each s, 3H, ring-CH_3 of HPPH), 2.87–3.10 (m, 8H, 4H for −NHCH_2(CH_2)$_2$$CH_2$NH-,4H for 2X – N($CH_2$)$_3$$CH_2SO_3$ of cyanine dye), 2.82 (m, 4H, cyclohexene $CH_2CH_2CH_2$), 2.2–2.3, 2.4–2.6 (each m, 2H, 17-CH_2CH_2CO- of HPPH), 1.92–2.08 (overlapped m, 13H, 3H for 31-CH_3 of HPPH, 8H for 2X – $NCH_2(CH_2)_2CH_2SO_3$, 2H for cyclohexene CH2CH2CH2), 1.6–1.8 (overlapped m, 20H, 3H for 18-CH_3 of HPPH, 12H for 4× CH_3 of cyanine dye, 2H for OCH_2CH_2(CH_2)$_3$$CH_3$ of HPPH, 3H for 8-CH_2CH_3 of HPPH), 1.1–1.4 (m, 10H, 6H for –O(CH)$_2$(CH_2)$_3$$CH_3$ of HPPH, 4H for −NHCH_2(CH_2)$_2$$CH_2$NH-), 0.66 (m, 3H, -O($CH_2$)$_5CH_3$ of HPPH), 0.30 (br s, 1H, 21-H of HPPH), −1.97 (s, 1H, 23-H of HPPH). ^{13}C-NMR (100 MHz, $CDCl_3$ / CD_3OD, δ ppm): 195.6, 173.9, 173.7, 145.0, 139.2, 133.8/133.7, 131.9, 130.7, 128.4,128.0, 127.7, 125.5, 125.1, 122.0, 110.4, 104.1, 100.8, 92.9, 72.8, 69.70/69.67, 51.8, 51.0, 50.4, 31.9, 31.6, 30.8, 30.1, 29.6, 29.3, 27.23/27.22, 26.41/26.32, 26.26/26.23, 26.0, 24.48/24.42, 22.9, 22.6, 22.5, 22.30/22.28, 19.4, 17.3, 13.8, 11.8, 11.1, 10.9. Mass: m/z calculated for $[M+H]^+$ $C_{96}H_{111}N_8O_{10}S_3$: 1632.7517, found HRMS $[M+H]^+$ 1632.7648

Conjugate 4—HPPH-N-Boc hexyldiamine (38.0 mg, 0.052 mmol) was taken in a dry round bottom flask (RBF), (50.0 ml) and stirred with 50% TFA/DCM (5.0 ml) at RT for 3 hr. Resultant mixture was concentrated and dried under high vacuum to remove trace of TFA. The crude thus obtained was dissolved in anhydrous DMF (25 ml) and cyanine dye (50.0 mg, 0.052 mmol), BOP (30.0 mg, 0.067 mmol) and triethylamine (3–4 drops) were added and the resultant mixture was stirred for 12 hr at room temperature under N_2 atmosphere. Solvent was removed under vacuum and the product was purified over

preparative plates using 15 % methanol-dichloromethane to give the final product, black solid, in a 35% yield. UV-Vis λ_{max} (in MeOH): 838.1 nm (ε 2.23 × 10^5), 661.0 nm (ε 5.34 × 10^4), 609.0 nm (ε 1.02 × 10^4), 538 nm (ε 8.79 × 10^4), 408 nm (ε 9.07 × 10^4); ^{1}H-NMR (400 MHz, CD_3OD, δ ppm): 9.76/9.75 (s, 1H, H-5 of HPPH), 9.34 (br s, 1H, HPPH H-10), 8.57–8.64 (overlapped m, 3H, 1H for H-20 of HPPH & 2H for −CH=C<u>H</u>-C=C-C=C<u>H</u>-CH=C-), 7.88, 7.73, 7.68, 7.54, 7.40, ~7.26, ~7.25, 6.99 (8× m, 16H, 12H for aromatic protons of cyanine dye & 4H for aromatic protons of phenyl thioether group), 6.08/6.09 (d, 2H, −C<u>H</u>=CH- C=C-C=CH-C<u>H</u>=C-, J=14.2 Hz), 5.93 (q, 1H, 3^1-H of HPPH, *J*=6.6 Hz), 5.08 (d, 1H, 13^1-C<u>H</u>H of HPPH, *J*=19.9 Hz), ~4.83 (overlapped d, 1H, 13^1-CH<u>H</u> of HPPH), 4.42 (q, 1H, 18-H of HPPH, *J*=7.2 Hz), 4.11 (br d, 1H, 17-H of HPPH, *J*~8 Hz), 3.53–3.78 (overlapped m, 11H, 4H for – $OCH_2(CH_2)_4CH_3$ & 8-CH_2CH_3 of HPPH, 3H for ring-CH_3 of HPPH, 4H for 2× – $NCH_2(CH_2)_3SO_3$),3.37 (s, 3H, ring-CH_3 of HPPH), 3.21 (s, 3H, ring-CH_3 of HPPH), 2.68–2.90 (overlapped m, 12H, 4H for 2× –$N(CH_2)_3CH_2SO_3$, 4H for –$NHCH_2(CH_2)_4CH_2NH$–, 4H, cyclohexene −$CH_2CH_2CH_2$–), 2.47 (br m, 1H of 17-CH_2CH_2CO-), 2.30 (br m, 1H of 17-CH_2CH_2CO-), 2.09/2.12 (d, 3H, 3^1-CH_3 of HPPH, *J*=6.7 Hz), 1.84–2.22 (overlapped m, 12H, 2H of 17-CH_2CH_2CO- of HPPH, 2H for cyclohexene −$CH_2CH_2CH_2$–, 8H for 2× – $CH_2(CH_2)_2CH_2SO_3$), 1.57–1.80 (overlapped m, 20H, 3H for 18-CH_3 of HPPH, 12H for 4× CH_3 of cyanine dye, 2H for -$OCH_2C\underline{H}_2(CH_2)_3CH_3$ of HPPH,3H for 8-$CH_2C\underline{H}_3$ of HPPH), 1.1–1.4 (overlapped m, 14H, 6H for –$O(C\underline{H})_2(CH_2)_3CH_3$ of HPPH, 8H for −$NHCH_2(C\underline{H}_2)_4CH_2NH$-), 0.68 (m, 3H, -$O(CH_2)_5C\underline{H}_3$ of HPPH). ^{13}C-NMR (100 MHz, $CDCl_3$ / CD_3OD, δ ppm): 173.8, 160.8, 155.7, 150.9, 149.1, 145.2, 139.2, 136.3, 135.8, 133.77/133.62, 131.99/131.88, 130.7, 129.9, 128.3, 127.9, 127.67/127.61,126.9, 125.5, 125.17/125.09, 123.6, 121.9, 105.6, 100.80/100.69, 72.76/72.70, 69.6, 51.7, 51.0, 50.0, 44.3, 39.5, 39.0, 31.6, 30.79/30.75, 30.0, 29.6, 28.80/28.73, 27.3, 27.2, 26.7, 26.4, 26.31/26.27, 26.04/26.01, 25.9, 24.4, 23.7, 22.8, 22.4, 20.7, 19.3, 17.2, 13.7, 11.7, 11.0, 10.7. Mass: m/z calculated for $[M+H]^+$ $C_{98}H_{115}N_8NaO_{10}S_3$: 1661.7830, found HRMS (TOFMS) $[M+H]^+$ 1661.8020.

Conjugate 5—HPPH-1,2-ethylenediamine (96 mg, 0.1414 mmoles), CD_3COOH (68.3 mg, 0.0707 mmoles), BOP (40.7 mg, 0.0919 mmoles) and 3 drops triethyl diamine were combined with 10 ml anhydrous DMF in a two neck rbf under Argon atm. Mixture was stirred at room temperature for 12 h. Upon completion the reaction mixture was neutralized with 5 % acetic acid and DMF was removed by concentrating the mixture under high vacuum. The resultant slush was re-suspended in DCM and washed with brine (×3) the aqueous layer was washed with DCM until it was transparent. All the organic layers were combined, dried over Na_2SO_4 and concentrated under high vacuum. This was purified via flash column chromatography using a gradient of 5 – 20% MeOH: DCM to yield a black solid (Pure yield 50 %). UV-Vis λ_{max} (in MeOH): 843.0 nm (ε 1.36 × 10^5), 661 nm (ε 4.52 × 10^4), 410 nm (ε 6.62 × 10^4); ^{1}H NMR (400 MHz, DMSO-d_6, δ ppm): 9.73/9.74 (s, 1H, H-5 of HPPH), 9.68/9.69 (s, 1H, H-10 of HPPH), 8.72 (s, 1H, H-20 of HPPH), 8.55, 8.01, 7.93, 7.86, 7.61, 7.47, 7.38, 7.27, 7.13 (9 × m, 18H, 2H for −N<u>H</u>$(CH_2)_4$N<u>H</u>-, 12H for cyanine dye aromatic protons & 4H for phenyl thioether aromatic protons), 8.39/8.44 (d, 2H, −CH=CH-C=C-C=CH-CH=C-, *J*=14.2 Hz), 6.20/6.22 (d, 2H, – CH=CH-C=C-C=CH-CH=C-, *J*=14.2 Hz), 5.91/5.95 (q, 1H, 31-H of HPPH, *J*= 6.7 Hz), 5.07, 5.24 (2 × d, each 1H, 131-CH2 of HPPH, *J*= 20.2 Hz), 4.52 (m, 1H, 18-H of HPPH), 4.25 (m, 1H, 17-H of

HPPH), 4.10 (br m, 4H, 2 × –$NCH_2(CH_2)_3SO_3$), 3.40–3.80 (m, 4H, -$OCH_2(CH_2)_4CH_3$ & 8-CH_2CH_3 of HPPH), 3.19/3.20, 3.31/3.32, & 3.578/3.581 (each s, 3H, ring-CH_3 of HPPH), 3.15– 3.35 (m, 8H, 4H for −$NH(CH_2)_2NH$-, 4H for 2X –$N(CH_2)_3CH_2SO_3$ of cyanine dye), 2.71 (br m, 4H, cyclohexene $CH_2CH_2CH_2$), 2.07–2.22, 2.36–2.58 (each m, 2H, 17-CH_2CH_2CO- of HPPH), 1.85–2.07 (overlapped m, 13H, 3H for 31-CH3 of HPPH, 8H for 2X – $NCH_2(CH_2)_2CH_2SO_3$, 2H for cyclohexene $CH_2C\underline{H}_2CH_2$), 1.56–1.82 (overlapped m, 20H, 3H for 18-CH_3 of HPPH, 12H for 4× CH_3 of cyanine dye, 2H for -$OCH_2C\underline{H}_2(CH_2)_3CH_3$ of HPPH, 3H for 8-$CH_2C\underline{H}_3$ of HPPH), 1.40–1.54 (m, 2H, –$O(CH)_2C\underline{H}_2(CH)_2CH_3$ of HPPH), 1.08–1.18 (m, 4H, – $O(CH)_3(C\underline{H})_2CH_3$ of HPPH),0.66 (m, 3H, -$O(CH_2)_5C\underline{H}_3$ of HPPH), 0.21/0.22 (br s, 1H, 21-H of HPPH), −2.03/–2.04 (s, 1H, 23- H of HPPH). ^{13}C-NMR (100 MHz, $CDCl_3$ / CD_3OD, δ ppm): 197.3, 174.7, 173.34/173.28, 172.4, 167.76/167.74, 161.0, 155.6, 150.8, 150.08/149.99, 149.0, 145.09/145.03, 144.80/144.73, 141.4, 139.5, 139.2, 137.96/137.94, 137.3, 136.24/136.23, 135.23/135.20, 133.63/133.56, 133.38/133.33, 132.72/132.55, 131.75/131.74, 130.5, 129.82, 129.76, 127.9, 127.6, 125.35/125.31, 125.0, 124.4, 122.0, 110.2, 105.81/105.75, 103.9, 100.25/100.20, 97.6, 92.9, 72.72/72.70, 69.65/69.59, 51.88/51.84, 51.00/50.98, 50.4, 50.0, 47.8, 44.6, 40.1, 38.96/38.94,33.3, 31.60/31.58, 30.0, 29.6, 27.04/27.00, 27.00/26.96, 26.26/26.22, 25.95/25.92, 24.35/24.22, 22.9, 22.45/22.42, 22.3, 20.7, 19.3, 17.2, 13.74/13.70, 11.74/11.73, 11.05/11.03, 10.79/10.73. Mass: m/z calculated for $[M+H^+]$ $C_{94}H_{107}N_8O_{10}S_3$: 1605.7204, found HRMS $[M+H]^+$: 1605.7462.

Conjugate 6—HPPH-1,2-butanediamine (41 mg, 0.0559 mmoles), CD_3COOH (27 mg, 0.02795 mmoles), BOP (16 mg, 0.03634 mmoles) and 3 drops triethyl diamine were combined with 10 ml anhydrous DMF in a two neck rbf under Argon atm. Mixture was stirred at room temperature for 12 h. Upon completion the reaction mixture was neutralized with 5 % acetic acid and DMF was removed by concentrating the mixture under high vacuum. The resultant slush was re-suspended in DCM and washed with brine (×3) the aqueous layer was washed with DCM until it was transparent. All the organic layers were combined, dried over Na_2SO_4 and concentrated under high vacuum. This was purified via flash column chromatography using a gradient of 5 – 20% MeOH/DCM to yield a black solid (Pure yield 46 %). UV-Vis λ_{max} (in MeOH): 843 nm (ε 1.43 × 10^5), 661 nm (ε 4.54 × 10^4), 604.1 nm (ε 1.18 × 10^4), 408.1 nm (ε 7.45 × 10^5); ^{1}H-NMR (400 MHz, DMSO-d_6, δ ppm): 9.77/9.78 (s, 1H, H-5 of HPPH), 9.71 (s, 1H, H-10 of HPPH), 8.79 (s, 1H, H-20 of HPPH), 8.62 (d, 2H, −CH=C$\underline{H}$-C=C-C=C$\underline{H}$-CH=C-, *J*=14.3 Hz), 8.48, 8.07, 7.92, 7.65, 7.51, 7.37, 7.28 (7 × m, 18H, 2H for −N$\underline{H}$$(CH_2)_4N\underline{H}$-, 12H for cyanine dye aromatic protons & 4H for phenylthioether aromatic protons), 6.32 (d, 2H, −C$\underline{H}$=CH-C=C-C=CH- C$\underline{H}$=C-, *J*=14.3 Hz), 5.96 (q, 1H, 3^1-H of HPPH, *J*= 6.6 Hz), 5.07, 5.21 (2 × d, each 1H, 13^1-CH_2 of HPPH, *J*= 20.1 Hz), 4.55 (q, 1H, 18-H of HPPH, *J*~ 7 Hz), 4.27 (m, 1H, 17-H of HPPH), 4.19 (br m, 4H, 2 × –$NCH_2(CH_2)_3SO_3$), 3.43–3.79 (2 × overlapped m, 4H, -$OCH_2(CH_2)_4CH_3$ & 8- CH_2CH_3 of HPPH), 3.21, 3.36, & 3.60 (each s, 3H, ring-CH_3 of HPPH), 3.15–3.33 (overlapped m, 6H, 2H for −$NHCH_2(CH_2)_3NH$-, 4H for 2× –$N(CH_2)_3CH_2SO_3$ of cyanine dye), 2.93 (m, 2H, −$NH(CH_2)_3CH_2NH$-), 2.77 (br m, 4H, cyclohexene $CH_2CH_2CH_2$), 2.05–2.22, 2.39–2.65 (each m, 2H, 17-$C\underline{H}_2C\underline{H}_2CO$- of HPPH), 2.01 (m, 3H, 3^1-CH_3 of HPPH), 1.78–2.01 (overlapped m, 10H, 8H for 2× –$NCH_2(C\underline{H}_2)_2CH_2SO_3$, 2H for cyclohexene $CH_2C\underline{H}_2CH_2$), 1.54–1.78 (overlapped m, 24H, 3H for

18-CH_3 of HPPH, 12H for 4× CH_3 of cyanine dye, 2H for -$OCH_2C\underline{H}_2(CH_2)_3CH_3$ of HPPH, 3H for 8-$CH_2C\underline{H}_3$ of HPPH, 4H for −$NHCH_2(C\underline{H}_2)_2CH_2NH$-), 1.45 (m, 2H, – $O(CH)_2C\underline{H}_2(CH)_2CH_3$ of HPPH), 1.23 (br m, 4H, –$O(CH)_3(C\underline{H})_2CH_3$ of HPPH), 0.66 (m, 3H, –$O(CH_2)_5C\underline{H}_3$ of HPPH), 0.27 (br s, 1H, 21-H of HPPH), −1.97 (s, 1H, 23-H of HPPH). ^{13}C-NMR (100 MHz, $CDCl_3$ / CD_3OD, δ ppm): 197.1, 173.6, 173.38/173.35, 172.4, 167.3, 160.7, 155.5, 150.6, 150.08/150.03, 148.7, 144.92, 144.88, 139.37/139.35, 139.03/139.01, 137.79/137.77, 137.0, 136.0, 135.5, 135.39/135.36, 133.43/133.41, 133.36/133.34, 132.63/132.52, 131.6, 130.3, 129.6, 129.4, 129.3, 128.19/128.16, 127.63/127.61, 127.57/127.56, 127.35/127.33, 127.2, 125.5, 124.7, 123.9, 121.7, 110.2, 105.4, 103.7, 100.3, 97.3, 92.7, 72.53/72.48, 69.3, 51.5, 50.68/50.66, 50.2, 49.7, 47.5, 43.9, 39.47/39.45, 38.77/38.73, 32.7, 31.3, 30.7, 29.7, 28.66/28.62, 28.6, 26.75/26.73, 26.73/26.70, 26.02/25.98, 25.92/25.87, 25.85/25.79, 25.7, 22.5, 22.14/22.13, 22.1, 18.9, 16.8, 13.25/13.24, 11.2, 10.6, 10.30/10.29. Mass: m/z calculated for $[M+H]^+$ $C_{96}H_{111}N_8O_{10}S_3$: 1632.7617, found HRMS: 1632.7648.

Conjugate 7—HPPH-1,6-hexanediamine (134 mg, 0.1819 mmoles), CD_3COOH (87.9 mg, 0.09096 mmoles), BOP (52.3 mg, 0.1182 mmoles) and 3 drops triethyl diamine were combined with 10 ml anhydrous DMF in a two neck round bottom flask under Argon atm. Mixture was stirred at room temperature for 12 h. Upon completion the reaction mixture was neutralized with 5 % acetic acid and DMF was removed by concentrating the mixture under high vacuum. The resultant slush was re-suspended in DCM and washed with brine (×3) the aqueous layer was washed with DCM until it was transparent. All the organic layers were combined, dried over Na_2SO_4 and concentrated under high vacuum. This was purified via flash column chromatography using a gradient of 5 – 20% MeOH:DCM to yield a black solid (Pure yield, 48 %). UV-Vis λ_{max} (in MeOH): 838.0 nm (ε 1.80×10^5), 661.0 nm (ε 4.54×10^4), 409 nm (ε 7.85×10^4); ^{1}H NMR (400 MHz, DMSO-d_6, δ ppm): 9.78 (s, 1H, H-5 of HPPH), 9.72 (s, 1H, H-10 of HPPH), 8.75 (s, 1H, H-20 of HPPH), 8.61 (d, 2H, -CH=C$\underline{H}$-C=C-C=C$\underline{H}$-CH=C-, *J*=14.2 Hz), 8.48, 8.17, 7.94, 7.71, 7.65, 7.51, 7.37, 7.26, 6.90 (9 × m, 18H, 2H for −N$\underline{H}(CH_2)_4N\underline{H}$-, 12H for cyanine dye aromatic protons & 4H for phenyl thioether aromatic protons), 6.38 (d, 2H, -CH=CH-C=C-C=CH-CH=C-, *J*=14.2 Hz), 5.96 (m, 1H, 3^1-H of HPPH), 5.03, 5.19 (2 × d, each ^{1}H, 131-CH_2 of HPPH, *J*~ 19.4 Hz), 4.53 (q, 1H, 18-H of HPPH, *J*~ 7 Hz), 4.27 (br m, 4H, 2 × −$NCH_2(CH_2)3SO_3$), 4.19 (br m, 1H, 17-H of HPPH), 3.41–3.80 (2× overlapped m, 4H, -$OCH_2(CH_2)4CH_3$ & 8-CH_2CH_3 of HPPH), 3.13, 3.32, & 3.60 (each s, 3H, ring-CH_3 of HPPH), 3.21 (br m, 4H, 2× −$N(CH_2)_3C\underline{H}_2SO_3$ of cyaninedye),3.10–3.4 (overlapped m, 2H, $NHC\underline{H}_2(CH_2)_5NH$-), 2.94 (m, 2H, $NH(CH_2)_5C\underline{H}_2NH$-), 2.78 (br m, 4H, cyclohexene $C\underline{H}_2CH_2C\underline{H}_2$), 2.10–2.25, 2.37–2.70 (each m, 2H, 17-$C\underline{H}_2C\underline{H}_2CO$- of HPPH), 2.01 (br m, 3H, 3^1-CH_3 of HPPH), 1.80–2.00 (overlapped m, 10H, 8H for 2X −$NCH_2(C\underline{H}_2)_2CH_2SO_3$, 2H for cyclohexene $CH_2C\underline{H}_2CH_2$), 1.54–1.80 (overlapped m, 24H, 3H for 18-CH_3 of HPPH, 12H for 4× CH_3 of cyanine dye, 2H for -$OCH_2C\underline{H}_2(CH_2)_3CH_3$ of HPPH, 3H for 8-$CH_2C\underline{H}_3$ of HPPH, 4H for –$NHCH_2C\underline{H}_2(CH_2)_2C\underline{H}_2CH_2NH$-), 1.26–1.50(overlapped m, 6H, 2H for –$O(CH_2)_2C\underline{H}_2(CH_2)_2CH_3$ of HPPH, 4H for –$NH(CH_2)_2(C\underline{H}_2)_2(CH_2)_2NH$-), 1.22 (br m, 4H, –$O(CH)_3(C\underline{H})_2CH_3$ of HPPH), 0.65 (m, 3H, -$O(CH_2)_5C\underline{H}_3$ of HPPH), 0.25 (br s, 1H, 21-H of HPPH), −2.00 (br s, 1H, 23-H of HPPH). ^{13}C-NMR (100 MHz, $CDCl_3$/CD_3OD, δ ppm): 197.5, 173.5, 172.5, 160.77/160.74, 160.6, 155.8, 151.0, 150.4, 149.15/149.13,

145.3,141.62/141.57, 139.7, 137.4, 136.4, 135.8, 132.76/132.70, 129.7, 128.1, 105.67/105.66, 104.2, 97.88/97.82, 92.8, 72.87/72.82, 69.8, 51.8, 50.1, 48.0, 40.2, 39.0, 33.18/33.14, 31.7, 31.28/31.25, 30.96/30.92, 30.2, 29.7, 29.4, 28.8, 26.1, 25.8, 24.6, 23.0, 22.6, 19.4, 17.4, 13.9, 11.9, 11.2, 11.0. Mass: m/z calculated for $[M+H]^+$ $C_{98}H_{115}N_8O_{10}S_3$: 1661.7830, found HRMS $[M+H]^+$ 1661.8060.

Compound 8a: HPPH-NBOC-1,2-ethylenediamine (HPPH-NBOC-EDA)—HPPH (100 mg, 0.157 mmoles), N-Ethyl-N'-(3-dimethylaminopropyl) carboiimide hydrochloride (EDCI) (60 mg, 0.314 mmoles) and anhydrous dichloromethane (DCM) (20 ml) were combined in a 50 ml two neck rbf under Argon atm. Upon stirring the mixture for 30 minutes at room temperature (RT), 4-dimethylamino pyridine (DMAP) (38 mg, 0.314 mmoles) and NBOC-ethylenediamine (50 mg, 0.314 mmoles) were added. This was stirred for 12 hours at RT. A crude TLC (eluted in a gradient of 5 – 20 % acetone/DCM) of an aliquot of the mixture showed that the reaction was complete. Reaction was stopped by diluting with DCM and washing with brine. The aqueous layer (brine) was washed with DCM until it was clear. All organic layers were combined, dried over anhydrous sodium sulphate (Na_2SO_4) and concentrated under vacuum. Purification was conducted via flash column chromatography using silica gel and eluted using the same gradient used to elute the crude TLC to obtain a black solid, (Pure yield 51 mg, 42 %). UV-Vis λ_{max} (in MeOH): 659.9 nm, 503 nm, 407.1 nm. ^{1}H-NMR (400 MHz, $CDCl_3$, δ ppm) 9.79/9.78 (s, 1H, *meso*-H), 8.98/8.94 (s, 1H, *meso*-H), 8.52 (s, 1H, *meso*-H), 6.36 (br s, 1H, amide NH), 5.91 (m, 1H, $CH_3C\underline{H}$Ohexyl), 5.27 (d, 1H, 13^1-C$\underline{H}$H, J ~ 19.5 Hz), 5.03 (d, 1H, 13^1-CH$\underline{H}$, J ~ 19.5 Hz), 4.97 (br s, 1H, amide NH), 4.52 (m, 1H, 18-H), 4.27 (br m, 1H, 17-H), 3.75 – 3.40 (m, 4H, 8-$\underline{CH_2}CH_3$ & -OC$\underline{H_2}(CH_2)_4CH_3$), 3.38 (s, 3H, ring-$CH_3$), 3.28 (s, 3H, ring-$CH_3$), 3.20 (br s, 2H, – NHC$\underline{H_2}$), 3.09 (br s, 2H, NHC$\underline{H_2}$), 3.03/2.99 (s, 3H, ring-CH_3), 2.68 (br s, 1H, 17^1-C$\underline{H}$H), 2.44 (br s, 1H, 17^1- CH$\underline{H}$), 2.34 (m, 1H, 17^2-C$\underline{H}$H), 2.00 – 2.18 (m, 4H, C$\underline{H_3}$CH-Ohexyl & 17^2- C$\underline{H}$H), 1.68 – 1.82 (m, 5H, 18-CH_3 & -OCH_2C$\underline{H_2}(CH_2)_3CH_3$), 1.56 (m, 3H, 8-$CH_2C\underline{H_3}$), 1.40 (m, 2H, – O$(CH_2)_2C\underline{H_2}(CH_2)_2CH_3$), 1.22 −1.30 (m, 4H, -O$(CH_2)_3$(C$\underline{H_2}$)$_2CH_3$), 1.19 (s, 9H, -OC$(CH_3)_3$), 0.79 (m, 3H, -O$(CH_2)_5C\underline{H_3}$), 0.44 (brs, 1H, core NH), −1.62 (br s, 1H, core NH); ^{13}C-NMR (100 MHz, $CDCl_3$, δ ppm): 196.65/196.63, 173.3, 172.1, 160.5, 156.9, 155.5, 150.9, 149.1, 145.22/145.20, 141.7/141.6, 139.93/139.90, 137.6, 136.3, 135.9/135.8, 132.6/132.5, 130.1, 127.9, 106.1, 103.99, 98.2/98.1, 92.7, 79.6, 73.03/73.00, 69.9, 51.9, 50.2, 48.2, 40.6, 40.5, 33.2, 31.94/31.91, 30.7, 30.4, 28.3, 26.28/26.26, 24.92/24.86, 23.20, 22.77/22.75, 19.5, 17.5, 14.18/14.15, 11.7, 11.5, 11.2. Mass: m/z calculated for $[M]^+$ $C_{46}H_{62}N_6O_5$: 778.4782, found HRMS $[MH]^+$ 779.4851; low res (ESIMS) $[MH]^+$: 779.7

Compound 8: HPPH-1,2-ethylenediamine (HPPH-EDA)—HPPH-NBOC-EDA (100 mg, 0.128 mmoles) was stirred with 50 % TFA/ DCM (5.0 ml) in a dry 50 ml rbf at RT for 3 hrs. Excess TFA was removed by concentrating the mixture under high vacuum. The resultant slush was diluted with DCM and washed with brine (×3) in order to remove traces of TFA. Organic fraction was collected, dried over Na_2SO_4 and concentrated under high vacuum to yield a black solid (Pure yield 50.5 mg, 58 %). UV-Vis λ_{max} (in MeOH): 660 nm, 605 nm, 536 nm, 505 nm, 407.1 nm; ^{1}H-NMR (400 MHz, $CDCl_3$, δ ppm) 9.65 / 9.64 (s, 1H, *meso*-H), 8.41 (br s, 1H, *meso*-H), 8.37 (s, 1H, *meso*-H), 7.71/7.68 (s, 1H, amide-H), 5.87

(m, 1H, $CH_3C\underline{H}$Ohexyl), 5.51 (d, 1H, 13^1-C$\underline{H}$H, *J*=19.9 Hz), 4.67 (d, 1H, 13^1-CH$\underline{H}$, *J*=19.9 Hz), 4.45 (br m, 1H, 18-H), 4.03 (br s, 1H, 17-H), 3.45 – 3.75 (m, 7H, 8-C$\underline{H}_2CH_3$, -OC$\underline{H}_2(CH_2)_4CH_3$ & ring CH_3), 3.07–3.35 (m, 8H, 2 × ring-CH_3 & CH_2 of $NHCH_2CH_2NH_2$), 2.50 – 3.05 (3 × m, 5H, CH_2 of $NHCH_2CH_2NH_2$, 3H of 17-CH_2CH_2), 2.12/2.10 (d, 3H, 3^1-CH_3, *J* ~ 6.8 Hz), 1.63 – 1.85 (m, 3H, 1H of 17-CH_2CH_2 & –OCH_2C$\underline{H}_2(CH_2)_3CH_3$), 1.55 (br s, 3H, 18-$CH_3$), 1.42 (m, 2H, -O$(CH_2)_2C\underline{H}_2(CH_2)_2CH_3$), 1.15 –1.33 (m, 4H, -O$(CH_2)_3$(C$\underline{H}_2)_2CH_3$), 0.81/0.74 (distorted t, 3H, -O$(CH_2)_5$C$\underline{H}_3$), 0.01 (br s, 1H, core NH), −1.58/–1.61 (br s, 1H core NH); ^{13}C-NMR (100 MHz, $CDCl_3$, δ ppm): 197.82/197.81, 176.1, 172.7, 161.22/161.21, 155.4, 150.32/150.27, 148.7, 145.0/144.9, 141.8/141.7, 139.7/139.6, 136.6, 136.01/135.95, 135.7, 132.7/132.5, 128.3, 127.0, 105.6, 103.3, 97.9/97.7, 92.8, 73.0, 69.90/69.86, 51.8, 50.4, 48.5, 41.1, 37.52, 34.1/34.0, 32.0/31.9, 30.6, 30.5/30.4, 26.34/26.27, 24.9/24.7, 23.0, 22.8/22.7, 19.2/19.1, 17.3/17.2, 14.23/14.15, 11.5/11.4, 11.22/11.17, 10.2. Mass: m/z calculated for $[M]^+$ $C_{41}H_{54}N_6O_3$: 678.9059, found HRMS $[MH]^+$ 679.4346.

Compound 9a: HPPH-NBOC-1,4-butanediamine (HPPH-NBOC-BDA)—HPPH (100 mg, 0.157 mmoles), EDCI (60 mg, 0.314 mmoles) and anhydrous DCM (20 ml) were combined in a 50 ml two neck rbf under Argon atm. Upon stirring the mixture for 30 minutes at room temperature (RT), DMAP (38 mg, 0.314 mmoles) and NBOC-1,4-butanediamine (59 mg, 0.314 mmoles) was added. This was stirred for 12 hours at RT. A crude TLC (eluted in a gradient of 5 – 20 % acetone/DCM) of an aliquot of the mixture showed that the reaction was complete. The reaction was diluted with DCM and washed with brine. The organic layer was collected, dried over Na_2SO_4 and concentrated under vacuum. Purification was conducted via column chromatography using silica gel and eluted using the same gradient mentioned above to obtain a black solid (Pure yield 62.3 mg, 49 %). UV-Vis λ_{max} (in MeOH): 659.9 nm, 503 nm, 408.9 nm; ^{1}H-NMR (400 MHz, $CDCl_3$, δ ppm) 9.80/9.79 (s, 1H, *meso*-H), 9.09/9.07 (s, 1H, *meso*-H), 8.52 (s, 1H, *meso*-H), 5.91 (m, 1H, $CH_3C\underline{H}$Ohexyl), 5.58 (br s, 1H, amide NH), 5.10 (d, 1H, 13^1 -C$\underline{H}$H, *J*=19.7 Hz), 4.97 (d, 1H, 13^1-CH$\underline{H}$), 4.59 (br s, 1H, amide NH), 4.47 (br m, 1H, 18-H), 4.22 (br m, 1H, 17-H), 3.42 – 3.72 (cm, 4H, 8-C$\underline{H}_2CH_3$ & -OC$\underline{H}_2(CH_2)_4CH_3$), 3.38 (s, 3H, ring-$CH_3$), 3.28 (s, 3H, ring-$CH_3$), 3.14/3.16 (s, 3H, ring-CH_3), 2.96 (m, 2H, −NHC$\underline{H}_2$), 2.90 (m, 2H, −NHC$\underline{H}_2$), 2.46, 2.28, 2.18, 1.97 (4× br m, each 1H, 17-CH_2CH_2), 2.12 (d, 3H, C$\underline{H}_3$CH-Ohexyl, *J*=6.7 Hz), 1.65–1.85 (br overlapped m, 5H, 3H of 18-CH_3 and 2H for -OCH_2C$\underline{H}_2(CH_2)_3CH_3$), 1.58 (br m, 3H, 8-$CH_2C\underline{H}_3$), 1.35–1.50 (br m, 2H, -O$(CH_2)_2$C$\underline{H}_2(CH_2)_2CH_3$), 1.31 (s, 9H, -OC$(CH_3)_3$), 1.10–1.27 (br m, 8H, -O$(CH_2)_3$(C$\underline{H}_2)_2CH_3$ & −NHCH_2(C$\underline{H}_2)_2CH_2$NH-), 0.72–0.83 (br m, 3H, -O$(CH_2)_5$C$\underline{H}_3$), 0.39 (br s, 1H, core NH), −1.67 (br s, 1H, core NH); ^{13}C-NMR (100 MHz, $CDCl_3$, δ ppm): 196.5, 172.6, 172.1, 160.6, 156.3, 155.4, 150.9, 149.1, 145.22/145.20, 141.61/141.56, 139.93/139.91, 137.7, 136.3, 135.80/135.77, 132.55/132.46, 130.2, 128.13/128.11, 106.07/106.05, 104.1, 98.16/98.09, 92.8, 79.2, 73.0, 69.9, 51.8, 50.2, 48.2, 40.1, 39.2, 33.0, 31.93/31.91, 30.6, 30.4, 28.5, 27.6, 26.6, 26.28/ 26.26, 24.92/24.86, 23.2, 22.77/22.75, 19.5, 17.6, 14.18/14.15, 11.8, 11.5, 11.2. Mass: m/z calculated for $[M]^+$ $C_{48}H_{66}N_6O_5$: 806.5095, found HRMS $[MH]^+$ 807.5162.

Compound 9: HPPH-1,4-butanediamine (HPPH-BDA)—HPPH-NBOC-BDA (100 mg, 0.128 mmoles) was stirred with 50 % TFA/ DCM (5.0 ml) in a dry 50 ml two neck rbf

at RT for 3 hrs. Excess TFA was removed by concentrating the mixture under high vacuum. The resultant slush was diluted with DCM and washed with distilled water (×3) in order to remove traces of TFA. Organic fraction was collected, dried over Na_2SO_4 and concentrated under high vacuum to yield a black solid (Pure yield 74.3 mg, 85 %). UV-Vis λ_{max} (in MeOH): 660 nm, 604 nm, 536 nm, 505 nm, 408.9 nm; ^{1}H-NMR (400 MHz, $CDCl_3$, δ ppm) 9.66/9.63 (s, 1H, meso-H), 8.55 (br s, 1H, meso-H), 8.41 (s, 1H, meso-H), 7.51 (s, 1H, amide-H), 5.85/5.81 (q, 1H, $CH_3C\underline{H}$Ohexyl, *J*=6.8 Hz), 5.23 (d, 1H, 13^1-C$\underline{H}$H, *J*=19.5 Hz), 4.79 (d, 1H, 13^1-CH$\underline{H}$, *J*=19.5 Hz), 4.47 (br q, 1H, 18-H), 4.00 (br m, 1H, 17-H), 3.40 – 3.78 (m, 7H, 8-C$\underline{H}_2$CH$_3$, -OC$\underline{H}_2$(CH$_2$)$_4$CH$_3$ & ring-CH$_3$), 3.29/3.28 (s, 3H, ring-CH$_3$), 3.17 (br s, 2H, −NHC$\underline{H}_2$), 3.14/3.10 (s, 3H, ring-CH$_3$), 2.20 −3.03 (6× br m, 6H, -C$\underline{H}_2$NH$_2$ & 17-C$\underline{H}_2$C$\underline{H}_2$-), 2.09/2.05 (d, 3H, C$\underline{H}_3$CH-Ohexyl, *J*=6.6 Hz), 1.94 (br s, 2H, -CH$_2$N$\underline{H}_2$), 1.75 (m, 3H, 18-CH$_3$), 1.55–1.72 (cm, 9H, −NHCH$_2$(C$\underline{H}_2$)$_2$CH$_2$NH$_2$ & 8-CH$_2$C$\underline{H}_3$ & -OCH$_2$C$\underline{H}_2$(CH$_2$)$_3$CH$_3$), 1.10–1.50 (cm, 6H, -O(CH$_2$)$_2$(C$\underline{H}_2$)$_3$CH$_3$), 0.82/0.72 (distorted t, 3H, -O(CH$_2$)$_5$C$\underline{H}_3$), −1.50 (br s, 1H, core NH); ^{13}C-NMR (100 MHz, $CDCl_3$, δ ppm): 197.85/197.84, 174.2, 172.8, 160.95/160.91, 155.57/155.56, 150.20/150.14, 149.04/149.02, 145.13/145.04, 142.06/141.96, 139.94/139.91, 136.63, 136.20/136.13, 135.69/135.68, 132.92/132.77, 128.57/128.53, 126.88/126.86, 105.57/105.53, 103.15/103.11, 98.07/97.85, 93.0, 73.03/73.00, 69.95/69.86, 52.1, 50.2, 48.2, 40.0, 38.7, 34.2, 32.03/31.91, 30.91, 30.47/30.40, 26.36/26.25, 26.2, 25.0, 24.90/24.76, 23.0, 22.83/22.73, 18.88/18.79, 17.05/16.96, 14.24/14.13, 11.38/11.35, 11.17/11.12, 10.60/10.51. Mass: m/z calculated for $[M]^+$ $C_{48}H_{58}N_6O_3$: 706.4570, found HRMS $[MH]^+$ 707.4655.

Compound 10a: HPPH-NBOC-1,6-hexanediamine (HPPH-NBOC-HDA)—HPPH (100 mg, 0.157 mmoles), EDCI (60 mg, 0.314 mmoles) and anhydrous DCM (20 ml) were combined in a 50 ml two neck round bottom flask under argon. Upon stirring the mixture for 30 minutes at room temperature (RT), DMAP (38 mg, 0.314 mmoles) and NBOC-1,6-hexanediamine (68 mg, 0.314 mmoles) was added. This was stirred for 12 hours at RT. A crude TLC (eluted in a gradient of 5 – 20 % acetone/DCM) of an aliquot of the mixture showed that the reaction was complete. The reaction was diluted with DCM and washed with brine. The organic layer was collected, dried over Na_2SO_4 and concentrated under vacuum. Purification was conducted via column chromatography using silica gel and eluted using the same gradient mentioned above to obtain a black solid. (Pure yield 65 mg, 50 %). UV-Vis λ_{max} (in MeOH): 660 nm, 504 nm, 407.1 nm; ^{1}H-NMR (400 MHz, $CDCl_3$, δ ppm) 9.79/9.78 (s, 1H, *meso*-H), 9.21/9.19 (s, 1H, *meso*-H), 8.52 (s, 1H, *meso*-H), 5.91 (m, 1H, $CH_3C\underline{H}$Ohexyl), 5.44 (br s, 1H, amide NH), 5.21 (d, 1H, 13^1-C$\underline{H}$H, *J* = 19.5 Hz), 5.04 (d, 1H, 13^1 – CH$\underline{H}$, *J* = 19.5 Hz), 4.41–4.79 (br m, 2H, 18-H & amide NH), 4.30 (br s, 1H, 17-H), 3.50–3.53 (cm, 4H, 8-C$\underline{H}_2$CH$_3$ & -OC$\underline{H}_2$(CH$_2$)$_4$CH$_3$), 3.38 (s, 3H, ring-CH$_3$), 3.30 (s, 3H, ring-CH$_3$), 3.27 (s, 3H, ring-CH$_3$), 2.95 (br m, 4H, −NHC$\underline{H}_2$(CH$_2$)$_4$CH$_2$NH-), 2.62, 2.42, 2.21, 1.90 (4× br m, each 1H, 17-CH$_2$CH$_2$), 2.12 (d, 3H, C$\underline{H}_3$CH-Ohexyl, *J*~6.6 Hz), 1.78 (d, 3H, 18-CH$_3$, *J* = 7.1 Hz), 1.70–1.80 (m, 2H, -OCH$_2$C$\underline{H}_2$(CH$_2$)$_3$CH$_3$), 1.63 (m, 3H, 8-CH$_2$C$\underline{H}_3$), 1.4 (overlapped m, 2H, -O(CH$_2$)$_2$C$\underline{H}_2$(CH$_2$)$_2$CH$_3$), 1.35 (s, 9H, -OC(CH$_3$)$_3$), 1.00–1.32 (overlapped m, 12H, -O(CH$_2$)$_3$(C$\underline{H}_2$)$_2$CH$_3$ & −NHCH$_2$(C$\underline{H}_2$)$_4$CH$_2$NH-), 0.79 (distorted t, 3H, -O(CH$_2$)$_5$C$\underline{H}_3$), 0.45 (br s, 1H, core NH), −1.67 (br s, 1H, core NH); ^{13}C-NMR (100 MHz, $CDCl_3$, δ ppm): 196.4, 172.4, 172.1, 160.6, 156.2, 155.4, 150.9, 149.1, 145.2, 141.60/141.54, 139.92/139.89, 137.7, 136.4, 135.80/135.76, 132.53/132.45, 130.3,

128.14/128.12, 106.12/106.11, 104.1, 98.15/98.09, 92.8, 79.1, 73.02/72.99, 69.9, 51.9, 50.2, 48.2, 40.3, 39.2, 33.0, 31.92/31.91, 30.59/30.58, 30.4, 30.0, 29.3, 28.5, 26.27/26.25, 26.2, 26.1, 24.91/24.87, 23.3, 22.76/22.75, 19.6, 17.6, 14.17/14.15, 11.9, 11.5, 11.2. Mass: m/z calculated for $[M + H]^+$ $C_{50}H_{70}N_6O_5$: 835.5564, found HRMS $[M + H]^+$ 835.5451.

Compound 10: HPPH-1,6-hexanediamine (HPPH-HDA)—HPPH-NBOC-HDA (100 mg, 0.128 mmoles) was stirred with 50 % TFA/ DCM (5.0 ml) in a dry 50 ml round bottom flask (rbf) at RT for 3 hrs. Excess TFA was removed by concentrating the mixture under high vacuum. The resultant slush was diluted with DCM and washed with distilled water (×3) in order to remove traces of TFA. Organic fraction was collected, dried over Na_2SO_4 and concentrated under high vacuum to yield a black solid (yield 59.5 mg, 67 %). UV-Vis λ_{max} (in MeOH): 660 nm, 602 nm, 538.1 nm, 506 nm, 407.1 nm; ^{1}H-NMR (400 MHz, $CDCl_3$, δ ppm) 9.65/9.63 (s, 1H, meso-H), 8.41/840 (s,1H, *meso*-H), 8.30 (s, 1H, *meso*-H), 6.88 (br s, 1H, amide NH), 5.81/5.77 (q, 1H, $CH_3C\underline{H}$-Ohexyl, *J*=6.7 Hz), 5.15 (d, 1H, 13^1-C$\underline{H}$H, *J*=19.6 Hz), 4.87 (d, 1H, 13^1-CH$\underline{H}$, *J*=19.6 Hz), 4.42 (br m, 1H, 18-H), 4.07 (br m, 1H, H-17), 3.45–3.68 (cm, 4H, 8-C$\underline{H}_2$CH$_3$ & -OC$\underline{H}_2$(CH$_2$)$_4$CH$_3$), 3.26/3.24 (s, 3H, ring-CH$_3$), 3.15/3.13 (s, 3H, ring-CH$_3$), 3.07 (br s, 3H, ring-CH$_3$), 2.98 (m, 2H, −NHC$\underline{H}_2$), 2.58, 2.44, 2.20, 1.79 (4× cm, 6H, 17-C$\underline{H}_2$C$\underline{H}_2$ & -C$\underline{H}_2$NH$_2$), 2.00/2.02 (d, 3H, C$\underline{H}_3$CH-Ohexyl, *J*=6.7 Hz), 1.49–1.74 (cm, 8H, -OCH$_2$C$\underline{H}_2$(CH$_2$)$_3$CH$_3$, 8-CH$_2$CH$_3$, 18-CH$_3$), 1.10–1.45 (overlapped m, 16H, -O(CH$_2$)$_2$(C$\underline{H}_2$)$_3$CH$_3$, -(NHCH$_2$(C$\underline{H}_2$)$_4$CH$_2$N$\underline{H}_2$), 0.73/0.75 (distorted t, 3H, -O(CH$_2$)$_5$C$\underline{H}_3$), 0.28 (br s, 1H, core NH), −1.62/–1.63 (br s, 1H, core NH); ^{13}C-NMR (100 MHz, $CDCl_3$, δ ppm): 197.2, 173.53/173.51, 172.5, 160.94/160.91, 155.58/155.57, 150.6, 149.0, 145.07/145.03, 141.81/141.71, 139.84/139.82, 137.1, 136.02/136.00, 135.99/135.95, 132.70/132.62, 129.30/129.29, 127.3, 105.68/105.66, 103.56/103.55, 98.03/97.86, 92.89/92.88, 72.9, 69.8, 51.91/51.90, 50.2, 48.3, 40.0, 39.2, 33.7, 31.92/31.90, 31.3, 30.4, 28.9, 27.4, 26.27/26.23, 26.0, 25.8, 24.82/24.74, 23.2, 22.76/22.73, 19.2, 17.28/17.24, 14.17/14.13, 11.40/11.39, 11.27/11.25, 11.16/11.11. Mass: m/z calculated for $[M]^+$ $C_{45}H_{62}N_6O_3$: 734.4883, found HRMS $[MH]^+$ 735.4984.

Formulation

The compounds investigated in this study were formulated in 1 % Tween-80 in D5W (5% dextrose solution).

Photophysical characterization

UV-Vis absorption spectra of compounds (MeOH solutions) were acquired using a Shimadzu UV-3600 spectrophotometer. Fluorescence spectra were recorded using a Fluorolog-3 spectrofluorometer or a SPEX 270M Spectrometer (Jobin Yvon, Longjumeau, France). The SPEX 270M Spectrometer was utilized for measurements in NIR range; laser lines from Argon ion laser (Spectra Physics) or laser diodes emitting at 630 and 785 nm was used as excitation. Singlet oxygen, $^1O_2^*$, generation was detected by its phosphorescence emission signal at 1270 nm. A SPEX 270M Spectrometer equipped with Hamamatsu IR-PMT was used for recording singlet oxygen phosphorescence spectra. The sample placed in a quartz cuvette was positioned directly in front of the entrance slit of the spectrophotometer, and the emission signal was collected at 90° relative to the excitation laser beam. Additional long-pass filters [a 950 LP filter and a 538 AELP filter (both from Omega Optical)] were

used to attenuate the scattered light and fluorescence from the samples. $^1O_2{}^*$ phosphorescence decays at 1270 nm was acquired using Infinium oscilloscope (Hewlett-Packard) coupled to the output of the PMT. A second harmonic (532 nm) from a nanosecond pulsed Nd: YAG laser (Lotis TII, Belarus) operating at 20 Hz was used as the excitation source in this case.

In vitro tumor models

Colon-26 cells were grown in sterile RPMI-1640, 1× with L-glutamine with 10 % Fetal Calf Serum (FCS) (Atlanta Biologicals, triple 0.1μm filtered, Lawrenceville, GA), and 1 % Penicillin/Steptomycin/L-glutamine (P/S/*L*-G 10,000 I.U/ml penicillin, 10,000 mg/ml streptomycin, 29.2 mg/ml L-glutamine) was maintained in 5 % CO_2, 95 % air and 100 % humidity. U87, gliobastoma astrocytoma, cells were grown in Medium Essential Medium Eagle (MEM), 1× with Earle's Salt and L-glutamine, sterile with 10 % FCS, 1 % P/S/*L*-G, 1 % MEM Non-Essential Amino Acids 100× solution, sterile, 1 % Sodium Pyruvate, 100 mM solution, sterile, and 1% P/S/*L*-G and maintained in 5 % CO_2, 95 % air and 100 % humidity. All reagents, except FCS, but including Trypsin/EDTA, 1× (0.25 % Trypsin / 2.21 mM EDTA in HBSS without sodium bicarbonate, calcium and magnesium, sterile, Porcine Parvovirus tested) and DPBS, 1× (Dulbecco's Phosphate Buffered Saline), without calcium and magnesium, sterile were purchased from MediaTech, Inc., Manassas VA 20109. The 96 and 6 well plates were purchased from VWR. The MTT (3-[4,5-dimethylthiazol-2-yl]-2,5-diphenyltetrazolium bromide) cell viability assays were read on a microtiter plate reader at an absorbance of 560 nm. All compounds were formulated in 1 % Tween-80/D5W for solubility in aqueous solution and diluted in complete medium for all *in vitro* studies.

Determination of cell viability

MTT cell viability assays were conducted on **2–7** using the Colon-26 carcinoma cell line in two independent experiments with triplicates in each experiment. The plates were irradiated with a fluence of 4 J/cm^2 and fluence rate of 3.2 mW/cm^2 after 24 h incubation with the compounds. Colon-26 or U87 cells were seeded in rows three to eight of the 96 well plates at 5000 cells/well in 90 μl media and incubated with 10 μl of the stock PS-CD conjugate solutions at various drug concentrations ranging from 0 – 4 μM for 24 h. The experimental controls were placed in row one as 100 μl of media only and row two as 5000 cells in 100 μl of media only. Prior to irradiation the cells were washed and replaced with fresh media. Upon irradiation the cells were incubated 44 h at 37°C in the dark. The cells were later treated with 10 μl of 4.0 mg/ml solution of MTT dissolved in PBS. This was allowed to incubate for another 4 h. After 4 h the MTT was removed and 100 μl of dimethyl sulfoxide was added to solubilize the formazan crystals. The PDT efficacy was measured by reading the 96-well plate on a microtiter plate reader at an absorbance of 560 nm. The results were plotted with the corresponding drug dose at each fluence (J/cm^2) using the program OriginPro 8.6. The EC_{50} doses were calculated for each compound at the light dose of 4 J/cm^2 to compare their efficacy.

Animal and tumor models

Prior to commencement of *in vivo* studies all procedures or protocols were approved by the institutional animal care committee (IACUC). BALB/c mice 5–8 weeks of age were obtained from NCI Jackson Laboratory. The mice were inoculated subcutaneously (S.C.) on the right posterior shoulder with Colon-26 (1×10^6 in 50 μl medium) between 7–14 weeks of age. Athymic nude mice 6–8 weeks old obtained from Harlan were inoculated S.C. with U87, glioblastoma astrocytoma (2×10^6 in 50 μl medium). The mice were then used for *in vivo* studies when the tumors were 4–5 mm.

In vivo PDT treatment

Prior to inoculation with tumor cells the whole right side of the BALB/c mice were shaved and depilated with Nair. This was not needed when nudes were used. Upon reaching the appropriate treatment size (4–5 mm diameter) the mice were injected i.v. *via* tail vain with the conjugates. 24 hours post injection the mice were restrained in Plexiglass holders without anesthesia, treated with a 1.1 cm diameter area of drug-activating laser light at 665 nm and a fluence of 128 J/cm^2 and a fluence rate of 14 mW/cm^2.[39,40] The mice were observed daily after irradiation for tumor re-growth or tumor cure. Upon tumor recurrence measurements were taken using two orthogonal measurements Length and Width (perpendicular to L); volumes were calculated using formula $V = L*W^2/2$ and recorded. Mice were considered cured if there were no palpable tumors by day 60; however, if the tumors reached 400 mm^3 they were euthanized.

Tumor imaging

Three BALB/c mice per group bearing Colon-26 were imaged at three time points 24, 48 and 72 h after being anesthetized with Ketamine/Xylazine, delivered intraperitonally or anesthetized with isofluorane. Compounds were imaged using a Maestro GNIR Flex *In-vivo* imaging system using a broadband excitation at 710 – 740 nm and an 800 nm long pass emission.

Tumor uptake (*in vitro*)

In vitro cell uptake was determined by flow cytometry using an LSR II manufactured by Becton Dickson (BD). Colon-26 and U87 cells were seeded at 5.0×10^5 in 6 well plates in 2 ml complete media for 24 h. The conjugates were added at a concentration of 1 μM and incubated in the dark at 37°C for 24 h. Cells in each well were harvested and placed in 5 ml flow tubes with sieve caps, centrifuged cold at 4000 rpm at 10°C for 10 minutes. After removing the supernatant, the cells were re-suspended in cold 300 μl 2 % FCS in PBS (FCM Buffer), placed on ice then ran on a BD LSR II. BD FACSDiva software was used to setup the parameters and acquire the data for the experiment. Fluorescence was detected using the violet filter sets V 660/20, V 710/50 and V780/60. A variety of laser intercepts were used including the 405 nm Violet (25 mw Coherent Diode laser system), 488 nm Blue (20 mw primary laser, Coherent Solid State Laser system (Sapphire) and 640 nm Red (40 mw, Coherent “Cube” Solid State Laser system); however, for data analysis only those emission filter sets pertaining to the 405 nm Violet of 780/60, 710/50 and 660/20 nm were plotted

using Microsoft Excel after the data was generated via FCS Express 4.0 as Microsoft Powerpoint slides.

In vitro intracellular localization

Colon-26 and U87 cells were seeded in 35 mm glass bottom petri dishes at 1.25×10^5 and cultured in 2ml complete media for 24 – 48 h to allow for attachment and spreading. The PS-CD conjugates at concentrations of 0.25 μM, 0.5 μM, 1.0 μM and 2.0 μM were incubated in the dark at 37°C for 4 h and 24 h. Cells and drug mixtures were additionally incubated with organelle specific dyes such as Chloromethyl-X-rosamine (CMXRos) or MitoTracker Red (579/599) and FluoSpheres yellow/green (505/515) at concentrations of 2.5 nM and 1/10,000 from a 1/10 stock solution for 10 minutes and 24 h respectively. The organelle specific dyes were purchased from Molecular Probes (Eugene, OR). Prior to microscopy the media on the cells was removed and replaced with 1ml fresh media. A confocal microscope Leica TCS SP2 containing multiple laser lines and 3 acousto-optical detectors was used to observe the dyes; however, the excitation filters of 488, 543, and 633 nm were used to irradiate the organelle specific dyes pertaining to the lysosome, mitochondria, as well as the PS, HPPH, respectively.

Molecular Modeling Methods

The appropriate components of the conjugates were built by using standard bond length and bond angles using SYBYLX1.1 software package. Each component is first energy optimized by semi-empirical MO, PM3, and then components were connected by SYBYLX1.1. Finally, the complete conjugates were energy optimized by semi- empirical MO, PM3.

Conformational search on these conjugates was performed at the molecular mechanics level with the modified MMFF94s force field by MOE using stochastic conformational search with Monte Carlo and Molecular Dynamics as search engine. Under MOE, the low energy conformers were energy optimized under the modified MMFF94s force field during the search.

Supplementary Material

Refer to Web version on PubMed Central for supplementary material.

Acknowledgments

We are grateful to the NIH for financial support (RO1CA127369), the supplemental grant to promote diversity in health-related research to Nadine S. James RO1-S CA127369S. A partial funding from the program project grant PO1CA55791 and the RPCI's Cancer Center Support Grant from the NCI (P30CA016056) is also appreciated. This paper is dedicated to Dr. Janet Morgan, who suddenly passed away in 2014. We would also like to thank the Michigan State University, East Lansing, Michigan and the University at Buffalo, Amherst, NY, 14221 for the mass spectrometry analyses of new compounds.

REFERENCES

1. Veiseh M, Gabikian P, Bahrami SB, Veiseh O, Zhang M, Hackman RC, Ravanpay AC, Stroud MR, Kusuma Y, Hansen SJ, Kwok D, Munoz NM, Sze RW, Grady WM, Greenberg NM, Ellenbogen RG, Olson JM. Tumor Paint: A Chlorotoxin:Cy5.5 Bioconjugate for Intraoperative Visualization of Cancer Foci. Cancer Res. 2007; 67:6882–6888. [PubMed: 17638899]

2. Brem, H., Walter, KA., Tamargo, RJ., Olivi, A., Langer, R. Polym. Site-Specific Pharmacother. Domb, AJ., editor. Chichester, England: Wiley & Sons; 1994. p. 117139

3. Grossman SA, Reinhard C, Colvin OM, Chasin M, Brundrett R, Tamargo RJ, Brem H. The intracerebral distribution of BCNU delivered by surgically implanted biodegradable polymers. Journal of Neurosurgery. 1992; 76:640–647. [PubMed: 1545259]

4. Guerin C, Olivi A, Weingart JD, Lawson HC, Brem H. Recent advances in brain tumortherapy: local intracerebral drug delivery by polymers. Investigational New Drugs. 2004; 22:27–37. [PubMed: 14707492]

5. Tamargo RJ, Myseros JS, Epstein JI, Yang MB, Chasin M, Brem H. Interstitial chemotherapy of the 9L gliosarcoma: Controlled release polymers for drug delivery in the brain. Cancer Res. 1993; 53:329–333. [PubMed: 8417826]

6. Lesniak MS, Brem H. Targeted therapy for brain tumours. Nat. Rev. Drug Discovery. 2004; 3:499–508. [PubMed: 15173839]

7. Kostron H. Photodynamic diagnosis, therapy and the brain. Methods in molecular biology. Methods Mol. Biol. (Totowa, NJ, U. S.). 2010; 635:261–281.

8. Kamp MA, Santacroce A, Zella S, Reichelt DC, Felsberg J, Steiger H-J, Cornelius JF, Sabel M. Is it a glioblastoma? In dubio pro 5-ALA! Acta Neurochir (Wien). 2012; 154:1269. [PubMed: 22576268]

9. Beck TJ, Kreth FW, Beyer W, Mehrkens JH, Obermeier A, Stepp H, Stummer W, Baumgartner R. Interstitial photodynamic therapy of nonresectable malignant glioma recurrences using 5-aminolevulinic acid induced protoporphyrin IX. Lasers Surg Med. 2007; 39:386–393. [PubMed: 17565715]

10. Stepp H, Beck T, Pongratz T, Meinel T, Kreth F-W, Tonn JC, Stummer W. ALA and malignant glioma: fluorescence-guided resection and photodynamic treatment. J. Environ. Pathol., Toxicol. Oncol. 2007; 26:157–164. [PubMed: 17725542]

11. Stepp H, Beck T, Pongratz T, Meinel T, Tonn JC, Stummer W. Proc. SPIE-Int. Soc. Opt. Eng. 2006; 6078:60782W/1.

12. Stepp HG, Beck T, Beyer W, Pongratz T, Stroka R, Baumgartner R, Stummer W, Olzowy B, Mehrkens JH, Tonn JC, Reulen HJ. Proc. SPIE-Int. Soc. Opt. Eng. 2005; 5686:547.

13. Stummer W, Baumgartner R. Compr. Ser. Photochem. Photobiol. Sci. 2006; 7:155.

14. Stummer W, Novotny A, Stepp H, Goetz C, Bise K, Reulen HJ. Fluorescence-guided resection of glioblastoma multiforme by using 5-aminolevulinic acid-induced porphyrins: a prospective study in 52 consecutive patients. J. Neurosurg. 2000; 93:1003–1013. [PubMed: 11117842]

15. Stummer W, Pichlmeier U, Meinel T, Wiestler OD, Zanella F, Reulen H-J, Oppel F, Brune A, Lanksch W, Woiciechowsky C, Brock M, Vesper J, Tonn JC, Goetz C, Mayfrank L, Oertel MF, Seifert V, Franz K, Bink A, Schackert G, Pinzer T, Hassler W, Bani A, Meisel HJ, Kern BC, Mehdorn HM, Nabavi A, Brawanski A, Ullrich WW, Boeker DK, Winking M, Weber F, Langenbach U, Kaehler U, Arnold H, Knopp U, Grumme T, Stretz T, Stolke D, Wiedemayer H, Turowski B, Pietsch T. Fluorescence-guided surgery with 5-aminolevulinic acid for resection of malignant glioma: a randomised controlled multicentre phase III trial. Lancet Oncol. 2006; 7:392–401. [PubMed: 16648043]

16. Stummer W, Steiger H-J. Resection of glioblastoma. Journal of Neurosurgery. 2002; 96:809.

17. Bogaards A, Varma A, Zhang K, Zach D, Bisland SK, Moriyama EH, Lilge L, Muller PJ, Wilson BC. Fluorescence image-guided brain tumour resection with adjuvant metronomic photodynamic therapy: pre-clinical model and technology development. Photochem. Photobiol. Sci. 2005; 4:438442.

18. Lacroix M, Abi-Said D, Fourney DR, Gokaslan ZL, Shi W, DeMonte F, Lang FF, McCutcheon IE, Hassenbusch SJ, Holland E, Hess K, Michael C, Miller D, Sawaya R. A multivariate analysis of 416 patients with glioblastoma multiforme: prognosis, extent of resection, and survival. Journal of Neurosurgery. 2001; 95:190–198.

19. Kostron H, Obwegeser A, Jakober R, Zimmermann A, Rueck A. Use of texaphyrins in macrophage-mediated disease. Proc. SPIE-Int. Soc. Opt. Eng. 1998; 3247:40.

20. Zimmermann A, Ritsch-Marte M, Kostron H. mTHPC-mediated photodynamic diagnosis of malignant brain tumors. Photochem. Photobiol. 2001; 74:611–617. [PubMed: 11683042]

21. Agostinis P, Berg K, Cengel KA, Foster TH, Girotti AW, Gollnick SO, Hahn SM, Hamblin MR, Juzeniene A, Kessel D, Korbelik M, Moan J, Mroz P, Nowis D, Piette J, Wilson BC, Golab J. Photodynamic therapy of cancer: an update. CA Cancer J Clin. 2011; 61:250–281. [PubMed: 21617154]
22. Dougherty TJ, Gomer CJ, Henderson BW, Jori G, Kessel D, Korbelik M, Moan J, Peng Q. Photodynamic Therapy. J. Natl. Cancer Inst. 1998; 90:889–905. [PubMed: 9637138]
23. Henderson BW, Dougherty TJ. How does photodynamic therapy work? Photochem. Photobiol. 1992; 55:145–157. [PubMed: 1603846]
24. Henderson BW, Dougherty TJ, Malone PB. Studies on the mechanism of tumor destruction by photoradiation therapy. Progress in clinical and biological research. 1984; 170:601–612. [PubMed: 6241700]
25. Henderson, BW., Gollnick, SO. CRC Handbook of Organic Photochemistry and Photobiology. 2nd. Horspool, WM., Lenci, F., editors. Boca Raton: CRC Press LLC; 2004. p. 145/1
26. MacDonald IJ, Dougherty TJ. Basic principles of photodynamic therapy. J. Porphyrins Phthalocyanines. 2001; 5:105–129.
27. Chen Y, Gryshuk A, Achilefu S, Ohulchansky T, Potter W, Zhong T, Morgan J, Chance B, Prasad PN, Henderson BW, Oseroff A, Pandey RK. A novel approach to a bifunctional photosensitizer for tumor imaging and phototherapy. Bioconjugate Chem. 2005; 16:1264–1274.
28. James NS, Ohulchanskyy TY, Chen Y, Joshi P, Zheng X, Goswami LN, Pandey RK. Comparative tumor imaging and PDT Efficacy of HPPH conjugated in the mono-and di-forms to various polymethine cyanine dyes: part-2. Theranostics. 2013; 3:703–718. [PubMed: 24019855]
29. Lovell Jonathan F, Chen J, Jarvi Mark T, Cao W-G, Allen Annette D, Liu Y, Tidwell Thomas T, Wilson Brian C, Zheng G. FRET Quenching of Photosensitizer singlet oxygen generation. J. Phys. Chem. B. 2009; 113:3203–3211. [PubMed: 19708269]
30. Baba K, Pudavar HE, Roy I, Ohulchanskyy T, Chen Y, Pandey RK, Prasad PN. A New method for delivering a Hydrophobic Drug for Photodynamic Therapy Using Pure Nanocrystal Form of the Drug. Molecular Pharmaceutics. 2007; 2:289–297.
31. Gupta A, Wang S, Pera P, Rao KV, Patel R, Ohulchanskyy Tymish, Missert Joseph, Morgan J, Kopelman R, Pandey RK. Multifunctional nanoplatforms for fluorescence imaging and photodynamic therapy developed by post-loading photosensitizer and fluorophore to polyacrylamide (PAA) nanoparticles. Nanomedicine, N. M. B. 2012; 8:941–950.
32. Pandey RK, Sumlin AB, Potter WR, Bellnier DA, Henderson BW, Constantine S, Aoudia M, Rodgers MR, Smith KM, Dougherty TJ. Structure and Photodynamic Efficacy Among Alkyl Ether Analogues of Chlorophyll-a Derivatives. Photochem. Photobiol. 1996; 63:194–205.
33. Minnes R, Weitman H, You Y, Detty Michael R, Ehrenberg B. Dithisporphyrin derivatives as photosensitizers in membranes and cells. J Phys Chem B. 2008; 112:3268–3276. [PubMed: 18278897]
34. Silverman, RB. The Organic Chemistry of Drug Design and Drug Action. Burlington, USA: Elsevier Academic Press; 2004.
35. Thomas, G. Fundamentals of Medicinal Chemistry. New York, USA: John Wiley & Sons Ltd; 2003.
36. Gollnick SO, Evans SS, Baumann H, Owczarczak B, Maier P, Vaughan L, Henderson BW. Role of cytokines in photodynamic therapy-induced local and systemic inflammation. Br. J. Cancer. 2003; 88(11):1772–1779. [PubMed: 12771994]
37. Gollnick SO, Kabingu E, Kousis PC, Henderson BW. Stimulation of the host immune response by photodynamic therapy (PDT). Proceedings of SPIE-The International Society for Optical Engineering. 2004; 5319:60–70.
38. Gollnick SO, Liu X, Owczarczak B, Musser DA, Henderson BW. Altered expression of interleukin 6 and interleukin 10 as a result of photodynamic therapy in vivo. Cancer Research. 1997; 57(18): 3904–3909. [PubMed: 9307269]
39. Henderson BW, Busch TM, Snyder JW. Fluence rate as a modulator of PDT mechanisms. Lasers in surgery and medicine. 2006; 38:489–493. [PubMed: 16615136]
40. Snyder JW, Greco WR, Bellnier DA, Vaughan L, Henderson BW. Photodynamic Therapy: A Means to Enhanced Drug Delivery to Tumors. Cancer Research. 2012; 63:8126–8131.

41. Fingar VH, Kik PK, Haydon PS, Cerrito PB, Tseng M, Aband E, Wieman TJ. Analysis of acute vascular damage after photodynamic therapy using benzoporphyrin derivatives (BPD). Br. J. Cancer. 1999; 79:1702–1708. [PubMed: 10206280]

42. Gryshuk G, Chen Y, Potter W, Ohulchanskyy T, Oseroff A, Pandey RK. In vivo study and photodynamic efficacy of fluorinated photosensitizers derived from bacteriochlorophyll-a. J. Med. Chem. 2006; 49:1874–1881. [PubMed: 16539373]

43. Kessel D. Correlation between subcellular localization and photodynamic therapy. J. Porphyrins Phthalocyanines. 2004; 8:1009–1014.

44. Snyder CEJW, Ogilby PR, Gothelf KV. Control and selectivity of photosensitized singlet oxygen production: Challenges in complex biological systems. ChemBioChem. 2007; 8:475–481. [PubMed: 17323398]

45. Juzeniene A, Peng Q. Moan, Milestones in the development of photodynamic therapy and fluorescence diagnosis. J. Photochem. Photobiol. Sci. 2007; 6:1234–1245.

46. Kessel D, Luo Y. Photodynamic Therapy: A mitpchondrial inducer of apotosis. Cell Death Differ. 1999; 6:28–35. [PubMed: 10200545]

47. MacDonald IJ, Morgan J, Bellnier DA, Paszkiewicz GM, Whitaker JE, Litchfield DJ, Dougherty TJ. Subcellular localization patterns and their relationship to photodynamic activity of pyropheophorbide-a derivatives. Photochem. Photobiol. 1999; 70:789–797. [PubMed: 10568171]

48. Schneider R, Tirand L, Frochot C, Vanderesse R, Thomas N, Gravier J, Guillemin F, Barberi-Heyob M. Recent improvements in the use of synthetic peptides for a selective photodynamic therapy. Anti-Cancer Agents Med. Chem. 2006; 6:469–488.

49. Preedy, VR., editor. Apoptosis. Science Publishers, Inc.; 2010.

Highlights

- Development of efficient dual-function agents for cancer imaging and therapy.
- Tumor-avid chlorophyll-a-based compounds as delivery vehicle.
- A single agent for cancer imaging and therapy.
- The imaging and therapeutic moieties in the conjugate show similar PK/PD properties.

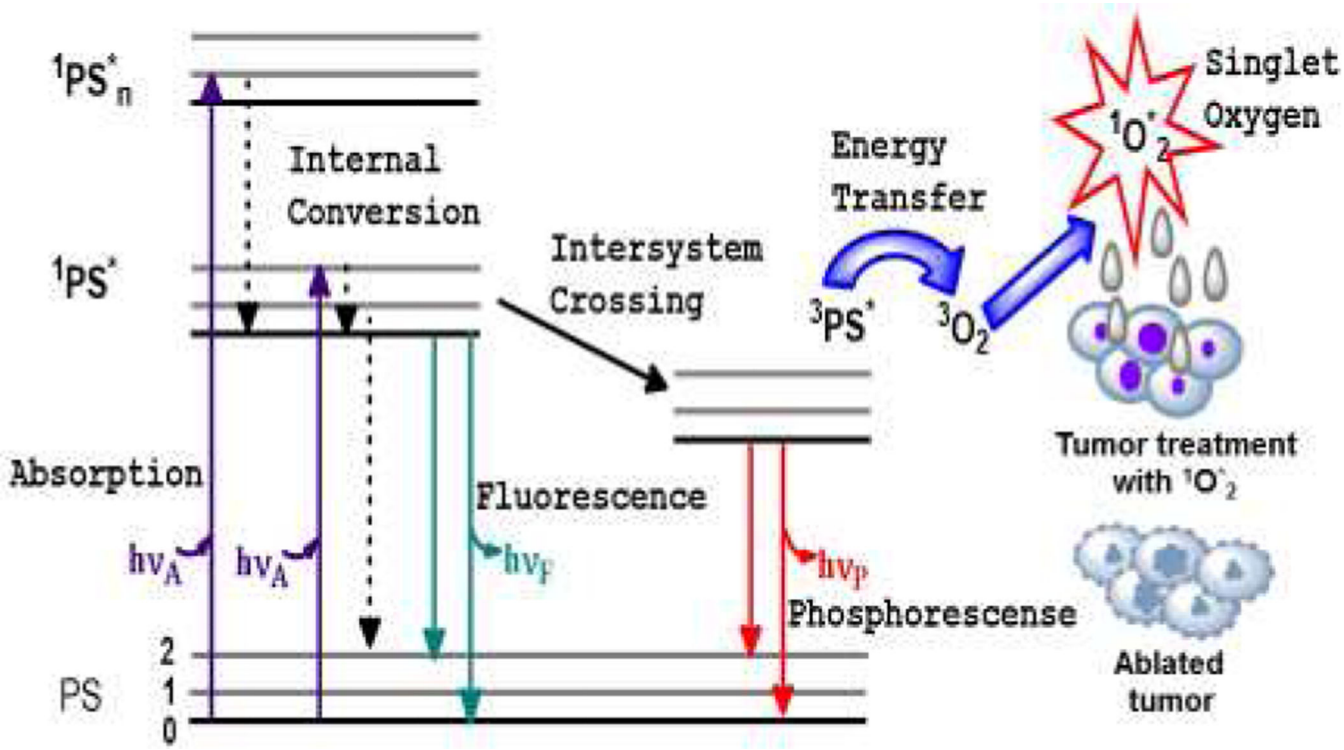

Figure 1.

Ablation of tumor cells after the three essential components (PS, light of the appropriate wavelength, and oxygen) of photodynamic therapy are combined. This usually results in the destruction of diseased tissue without affecting normal tissue. Jablonski diagram for the electronic states of the photosensitizer (PS) is shown on the left. Adopted from James et al.,[28] with permission.

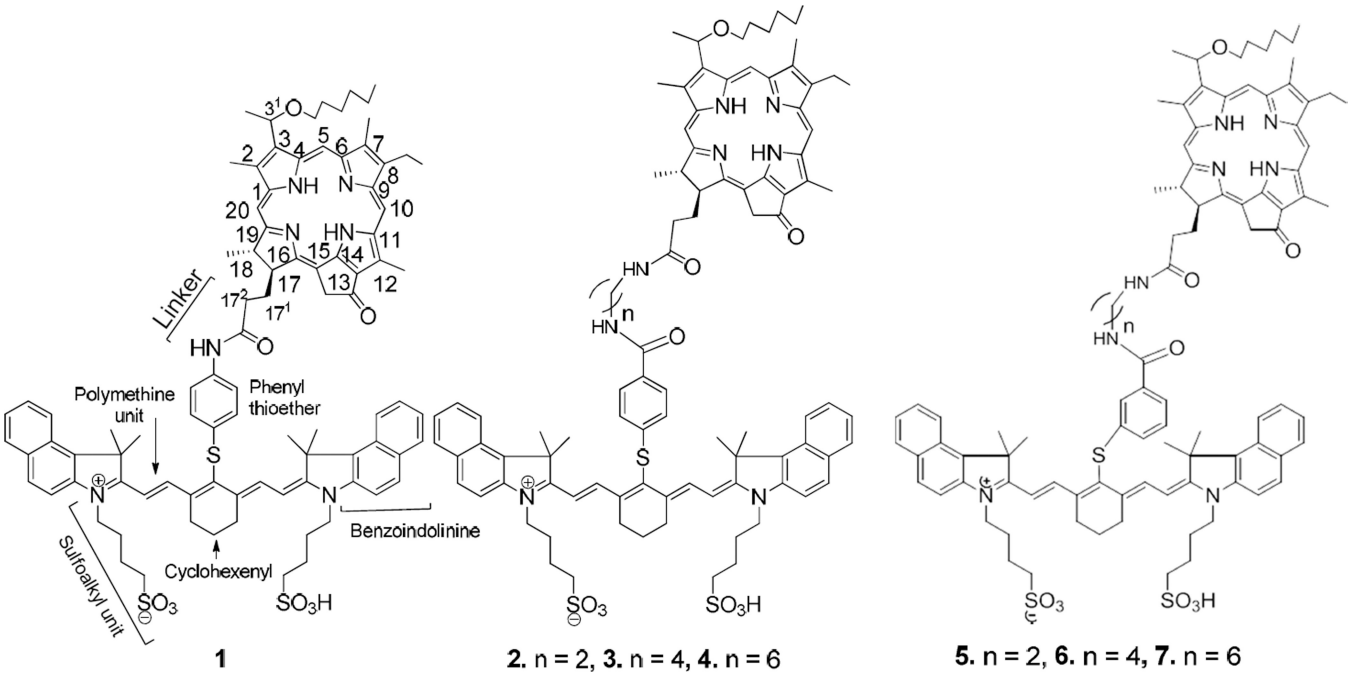

Figure 2.

Structures of HPPH-CD conjugates (lead compound **1**)[21] joined with variable length/ orientation of the linkers.

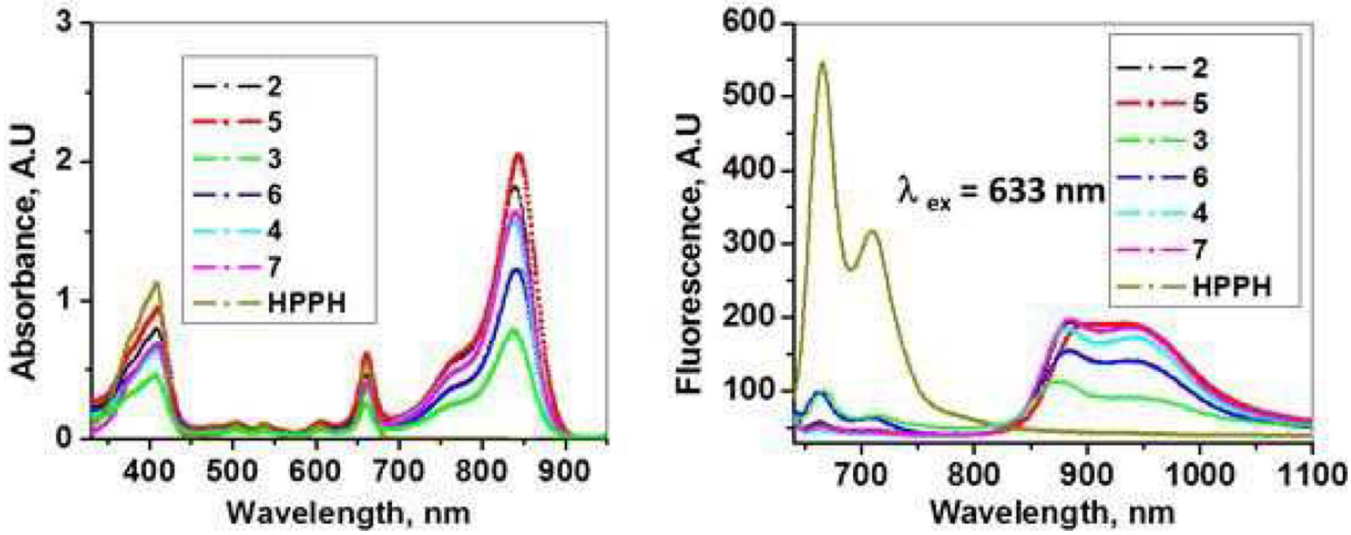

Figure 3.

Absorption (A) and fluorescence (B) spectra of HPPH and conjugates **2–7** (concentration: 5μM in methanol). Excitation of the conjugates at 633 nm (HPPH) shows significant difference in fluorescence intensity exhibited by the cyanine dye, suggesting the difference in overlap between the fluorescence of the HPPH and absorption peak of the cyanine dye moiety (FRET).

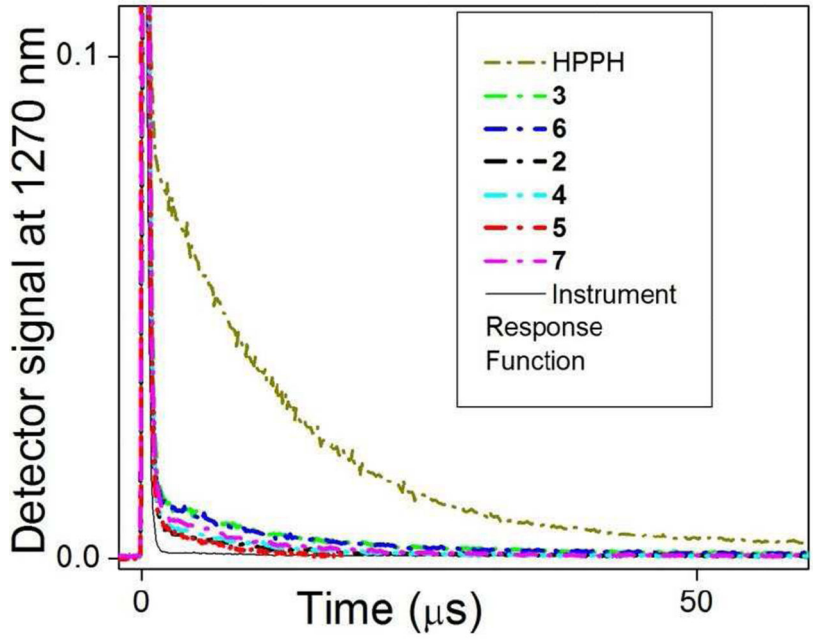

Compounds	Singlet Oxygen Yield (%)
HPPH	45
2	6
3	11
4	7
5	6
6	11
7	8

Figure 4.

Quantification of singlet oxygen sensitized by HPPH and conjugates **2–7**. The decays of the singlet oxygen phosphorescence at 1270 nm are shown on the left and the singlet oxygen yields obtained from the decays using HPPH as a reference[21] are on the right. Absorbance of the samples (methanol solutions) was matched at the wavelength of excitation (532 nm).

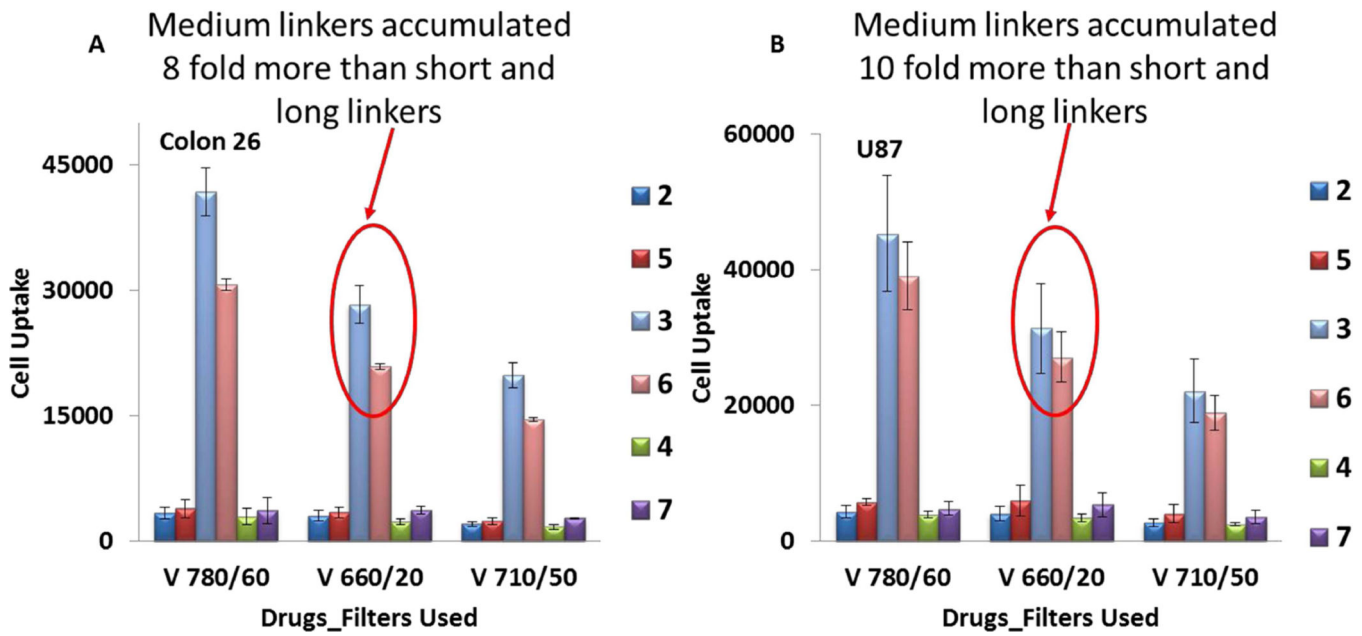

Figure 5.

Uptake of conjugates **2–7** in Colon-26 (A) and U87 cells (B), measured by flow cytometry. In both cell types the medium linked conjugates **3** and **6** accumulated 8-10 fold more than short and long linker conjugates (**2, 5** and **4, 7**, correspondingly).

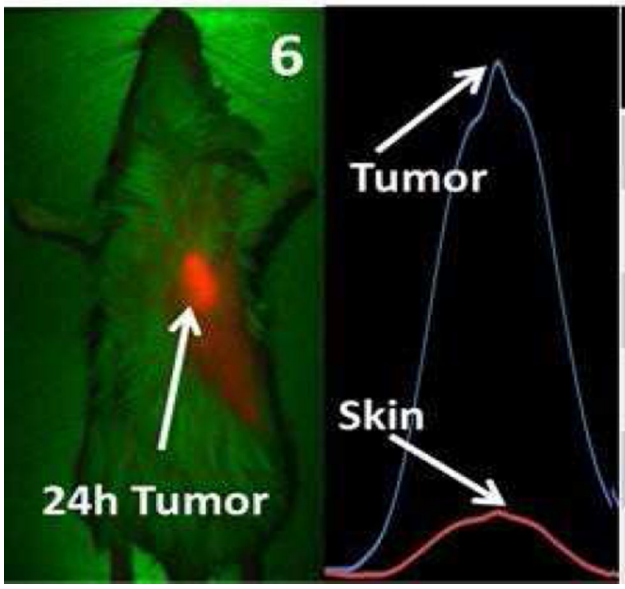

Drug	Tumor / Skin Ratio
2	2
3	10
4	2.3
5	2.5
6	6.5
7	2.5

Figure 6.

Left: Whole body image at 24 h post-injection of the conjugate **6** (0.3 μmol/kg)] of BALB/c mice bearing Colon-26 tumor. Middle: *In vivo* absorption spectra of **6** accumulated in tumor and skin measured by *in vivo* reflectance spectroscopy at 24 h post injection. Right: The tumor to skin/muscle ratios of the conjugates. The tumor to skin ratios were determined, *ex vivo* (BALB/c mice implanted with Colon-26 tumors) for each conjugate and the fluorescence intensities were averaged at the region of interest.

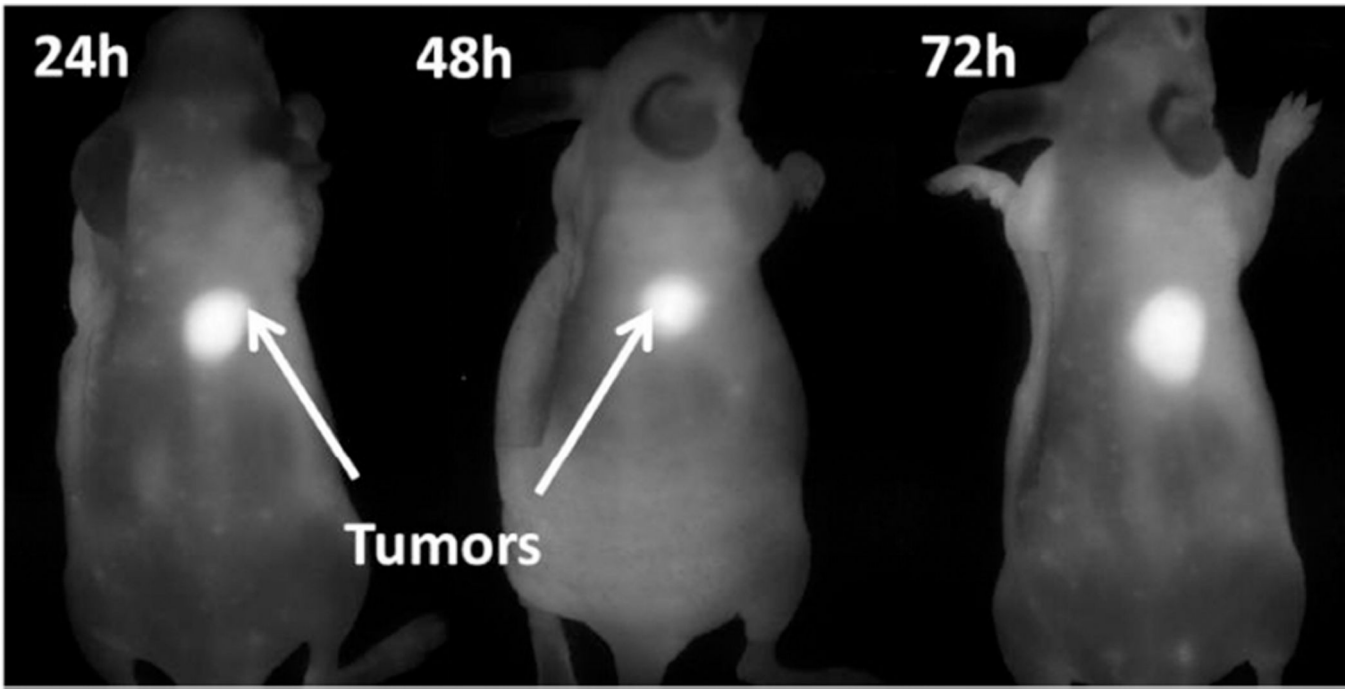

Figure 7.

Whole body near infrared fluorophore (CD) images of nude mice inoculated with U87 tumors with conjugate **6** (0.03 μmol/kg). Similar to BALB/c mice bearing Colon-26 tumors, the tumor uptake was significantly higher than surrounding skin/muscle in nude mice bearing U87 tumors at 24, 48 and 72 h post-injection (data not shown).

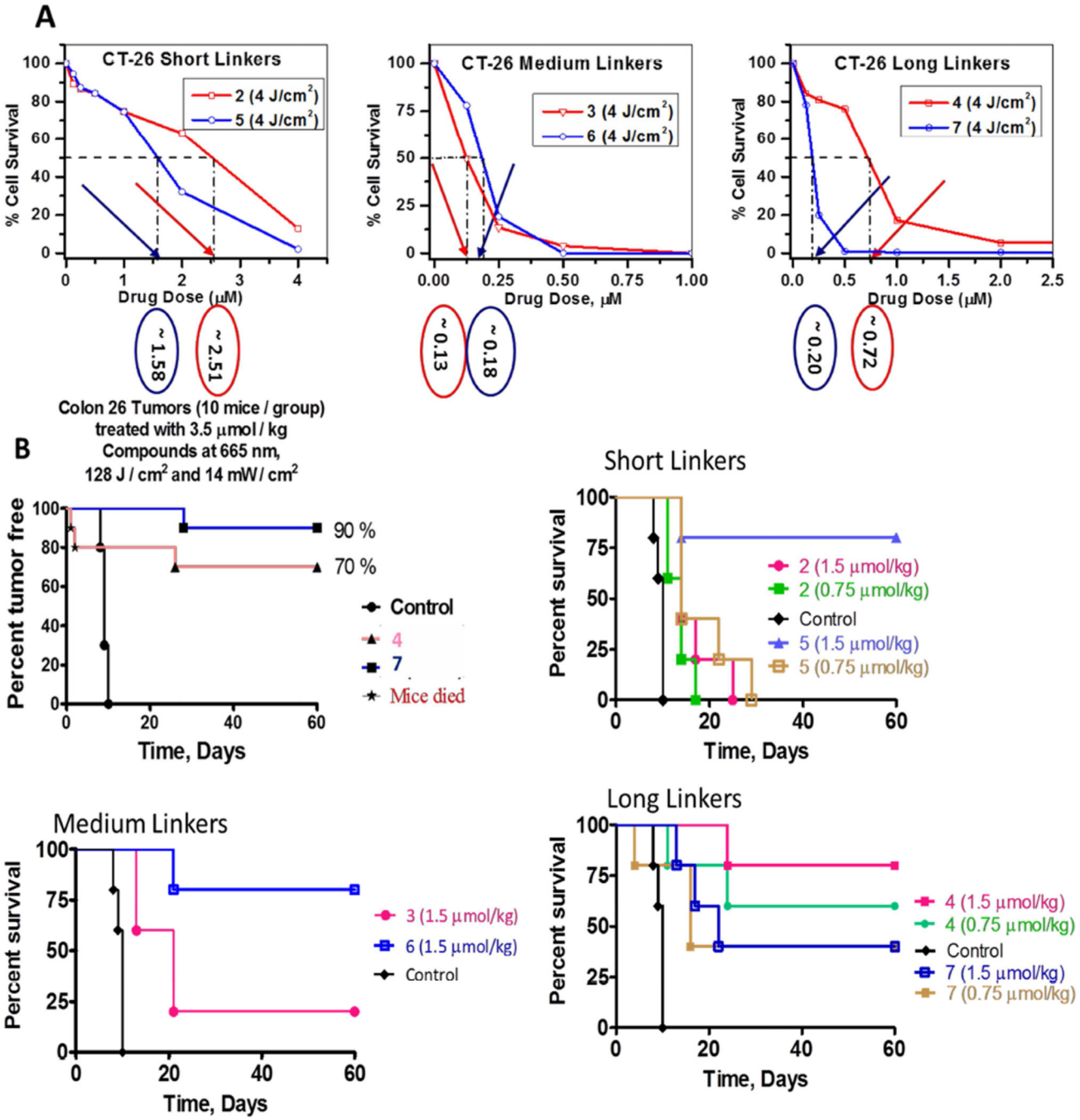

Figure 8.

A: MTT cell viability assays conducted on **2–7** using the Colon-26 carcinoma cell line were irradiated at a fluence of 4 J/cm^2 after 24 h incubation with the compounds. MTT was done at 48 h post-irradiation. The medium linkers **3** and **6** were more efficacious than the long and short linked compounds. The in vitro phototoxicity followed the order medium > long > short linked conjugates when their EC50 values were compared. **B:** In initial study the PDT efficacy of the conjugates was assessed at different drug doses, and the same light dose. The optimal drug dose was determined and the comparative efficacy of other conjugates was

determined at the similar treatment parameters (drug dose, 1.5 μmol/kg, light dose, 128 J/cm^2, 14 mW/cm^2) following the animal protocol approved by the institute's IACUC committee. The mice with no tumor re-growth at day 60 were listed in "complete cure" category. For *in vitro/in vivo* experiments, a tunable dye laser (Spectra-Physics, Mt. View, CA) was used as a light source.

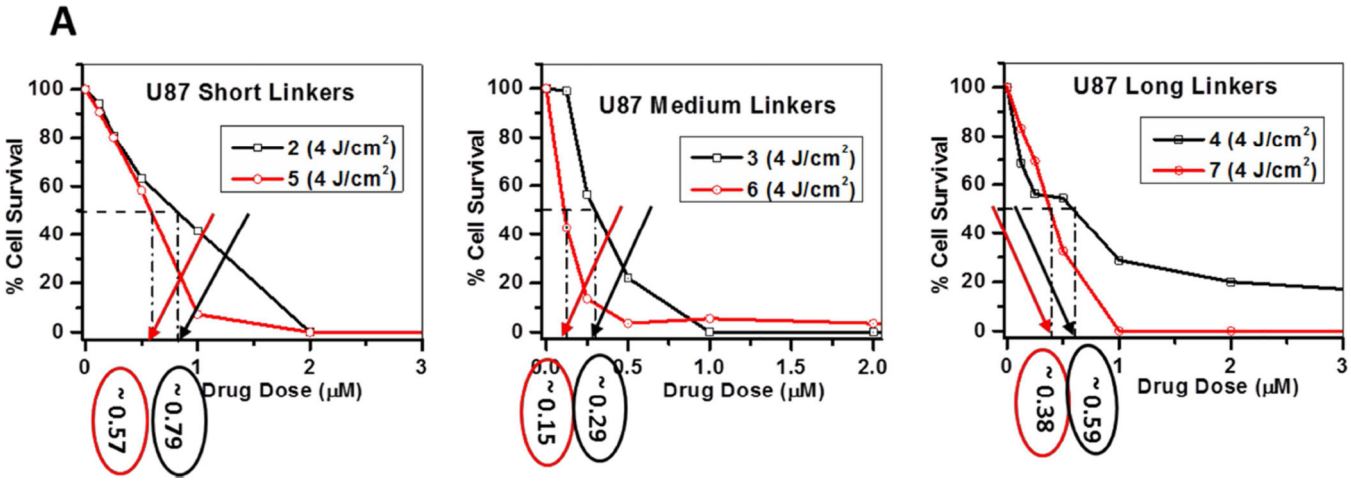

Figure 9.

MTT assay: A comparative *in vitro* photosensitizing efficacy of conjugates 2–7 in U87 cells and was in order of: **6**, EC_{50} 0.15 μM > **3**, EC_{50} 0.29 μM > **7**, EC_{50} 0.38 μM > **5**, EC_{50} 0.57 μM > **4**, EC_{50} 0.59 μM and > **2**, EC_{50} 0.79 μM.

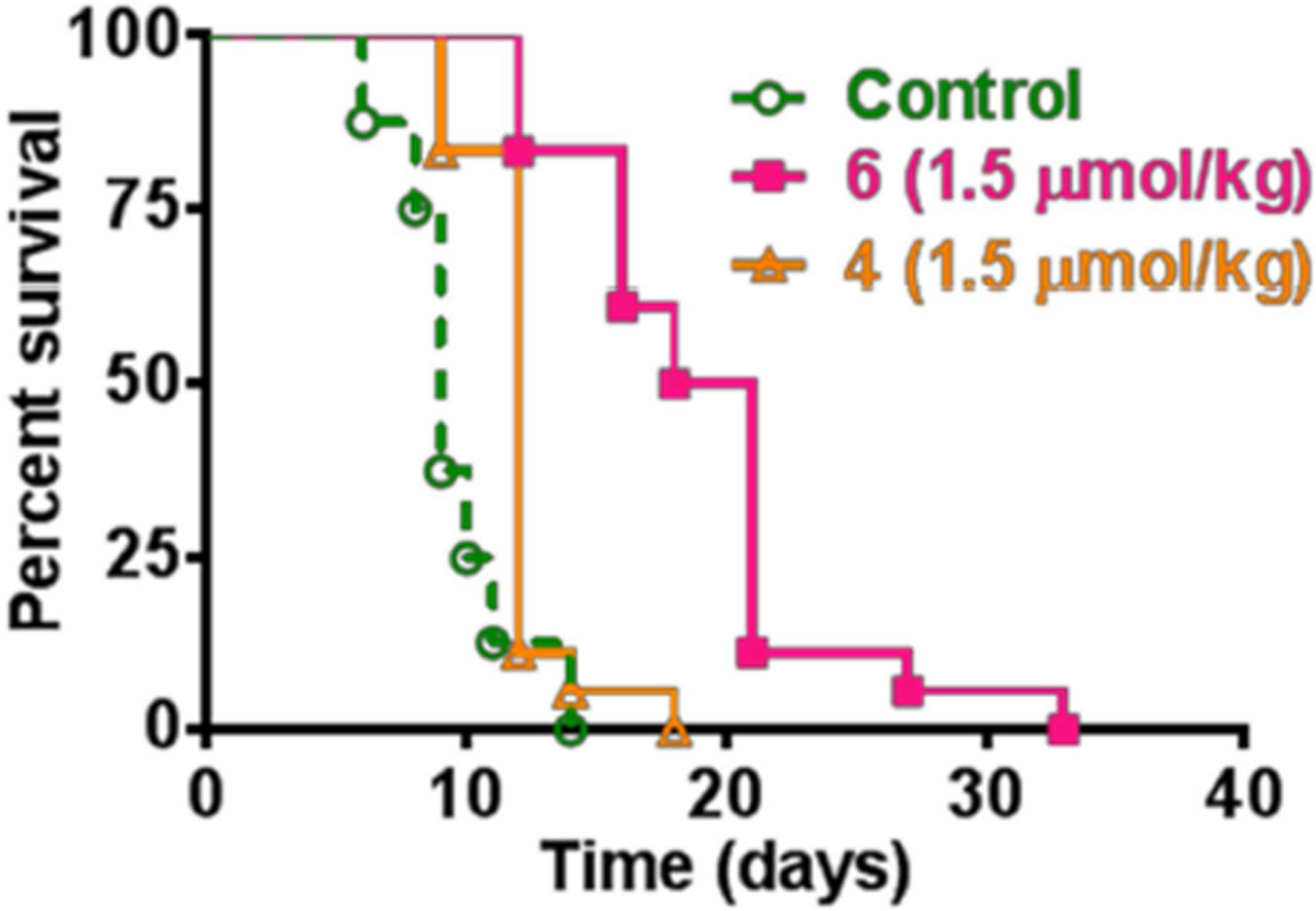

Figure 10.

Comparative *in vitro* PDT efficacy of the longer linked conjugate **4** and the medium linked conjugate **6** (dose: 1.5 μmol/kg) in nude mice bearing U87 tumors. The tumors were exposed to light (128 J/cm^2, 14 mW/cm^2)[39,40] at 24 h post-injection of the conjugates.

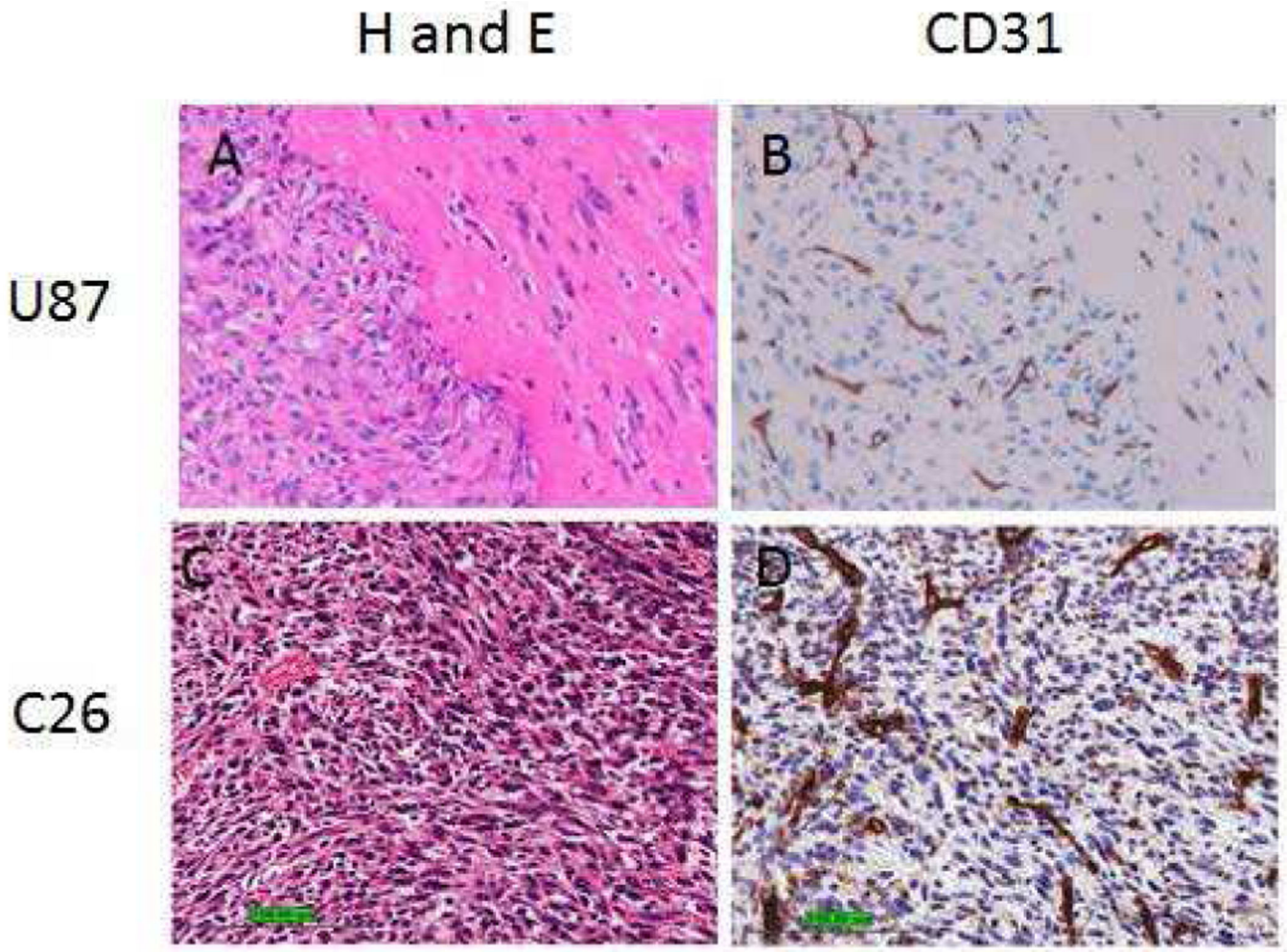

Figure 11.

Left Panel: Photomicrographs of U87 and Colon-26 (C26) tumors showing histology (H&E). Right Panel: Immunohistochemical staining to visualize micro vessels (CD31)

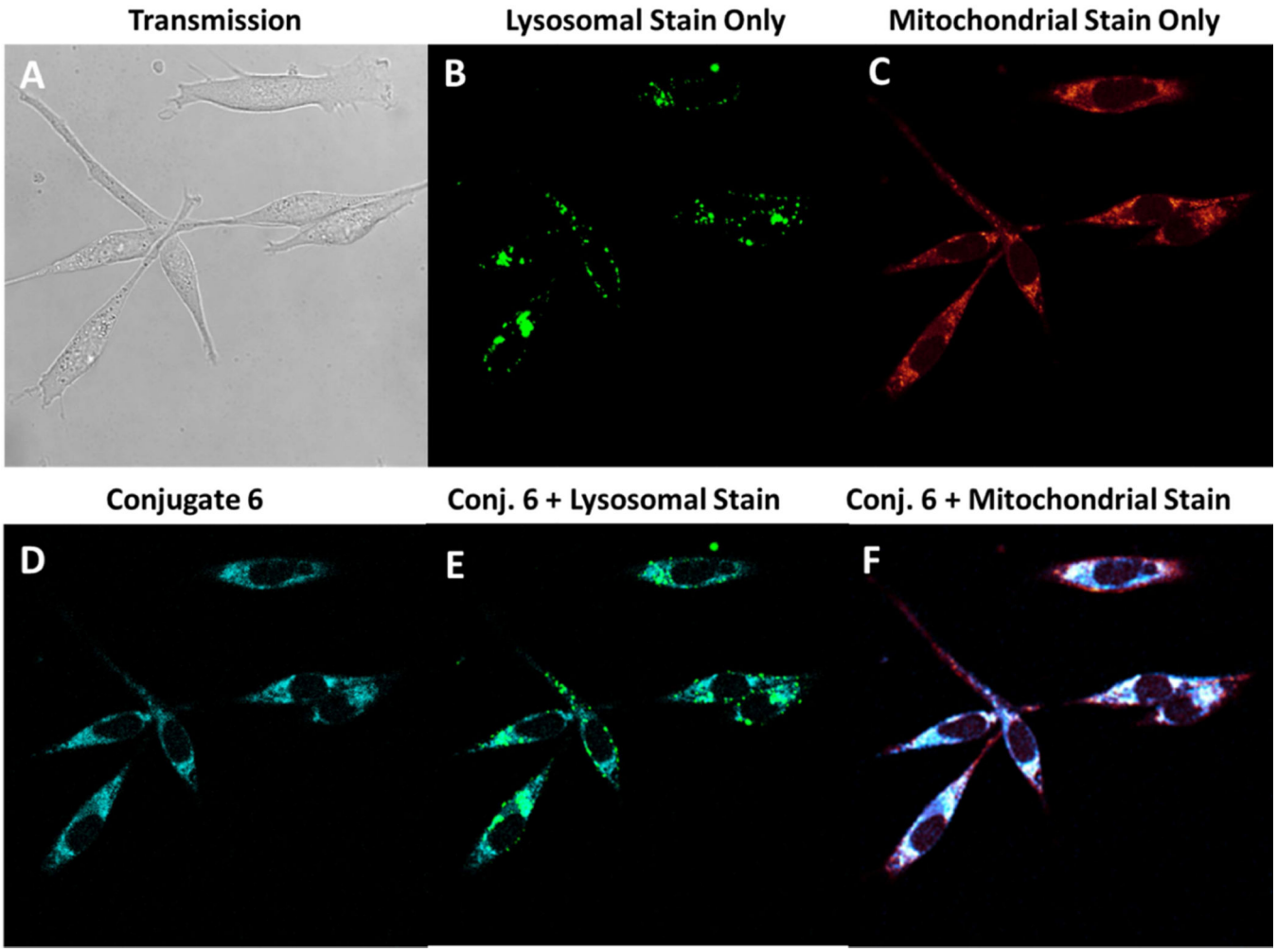

Figure 11A.

Localization of linked conjugates **6** in U87 cells at 1 μM. Images were taken 24h post incubation of the conjugates with the lysosomal dye, FluoSpheres ® yellow green, at a dilution of 1/100,000 from the commercial stock and following a 10 minutes incubation with the, mitochondrial dye, MitoTracker Red at 2.5 nM using a Leica TSP Confocal Microscope. Transmission (A), FluoSpheres ® yellow green (B), Mitotracker Red (C), *meta*-linked 4-carbon, conjugate **6** (D) Overlay of conjugate **6** with FluoSpheres ® yellow green (E) and Overlay of conjugate **6** with MitoTracker Red (F).

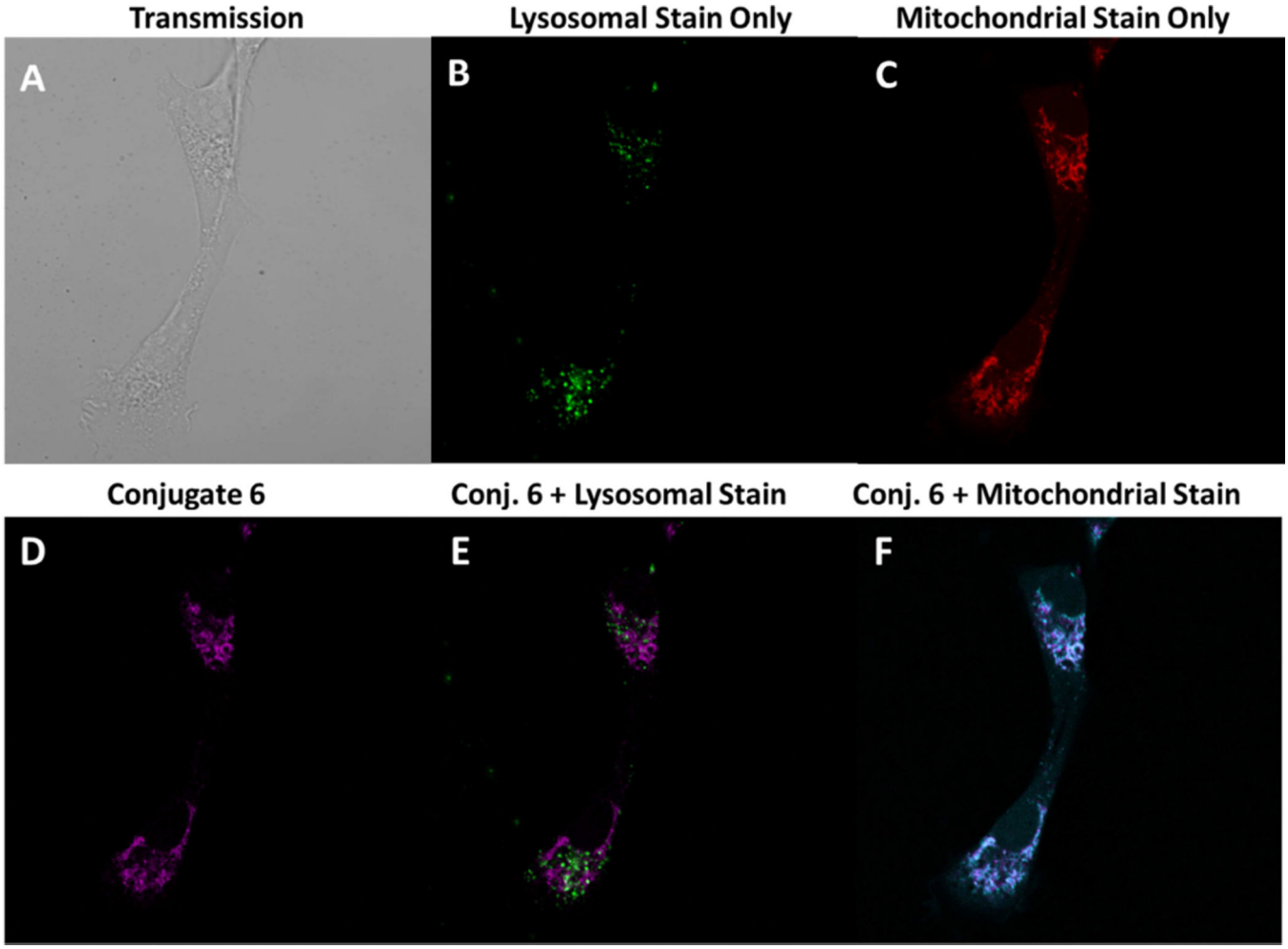

Figure 11B.

Localization of linked conjugate **6**, in Colon-26 cells at 1 μM. Images were taken 24h post incubation of the conjugates with the lysosomal dye, FluoSpheres ® yellow green, at a dilution of 1/100,000 from the commercial stock and following a 10 minutes incubation with the mitochondrial dye, MitoTracker Red, at 2.5 nM using a Leica TSP Confocal Microscope. Transmission (A), FluoSpheres ® yellow green (B), Mitotracker Red (C), *meta*-linked 4-carbon, conjugate **6** (D) Overlay of conjugate **6** with FluoSpheres ® yellow green (E) and Overlay of conjugate **6** with MitoTracker Red (F).

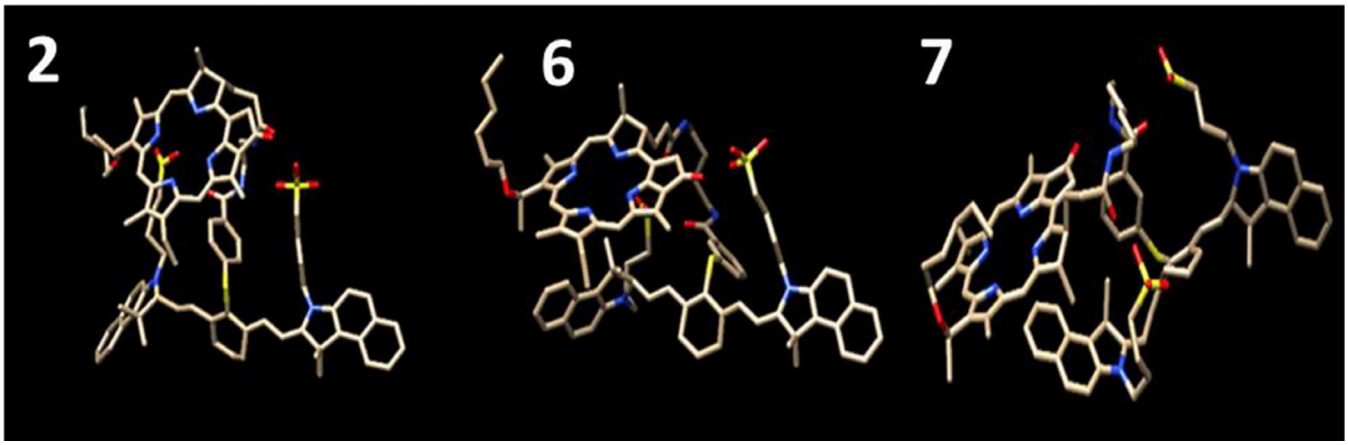

Figure 12.

Example of 3D structure of the modeled conjugates. The 3D models were built with SYBYL X1.1, and energy optimized with semi-empirical MO PM3. The conformational search with MOE2011.10 with stochastic Monte Carlo and Molecular Dynamics results in various conformations for all conjugates examined. Only some example for compound **2, 6** and **7** are shown in the figure.

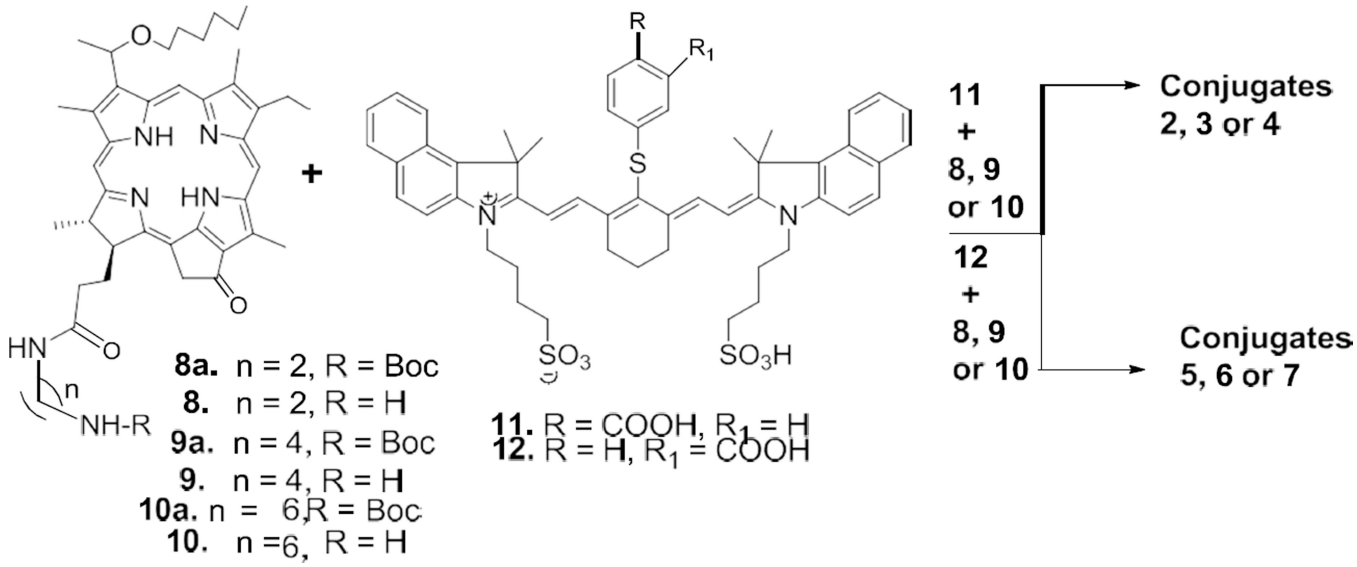

Scheme 1.

Synthesis of HPPH-CD conjugates in which the HPPH (photosensitizer) and the CD (fluorescence imaging agent) moieties are linked with variable number of carbon units.